Molecular Pharmacology Fast Forward. Published on December 1, 2008 as doi:10.1124/mol.108.051888
This article has not been copyedited and formatted. The final version may differ from this version.

MOL PHARM #051888

Knock-In Mouse Lines Expressing either Mitochondrial or Microsomal CYP1A1: Differing Responses to Dietary Benzo[*a*]pyrene as Proof-of-Principle

Hongbin Dong, Timothy P. Dalton, Marian L. Miller, Ying Chen,

Shigeyuki Uno, Zhanquan Shi, Howard G. Shertzer, Seema Bansal,

Narayan G. Avadhani and **Daniel W. Nebert***

Department of Environmental Health, and the Center for Environmental Genetics (**CEG**)
University Cincinnati Medical Center, Cincinnati OH 45267-0056

(H.D., T.P.D., M.L.M., Y.C., Z.S., H.G.S., D.W.N.)

Department of Biochemistry, Nihon University School of Medicine
30-1 Oyaguchikami-cho, Itabashi-ku, Tokyo 173-8610, Japan (S.U.)

Department of Animal Biology, School of Veterinary Medicine
University Pennsylvania, Philadelphia, PA 19104 (S.B., N.G.A.)

Molecular Pharmacology Fast Forward. Published on December 1, 2008 as DOI: 10.1124/mol.108.051888
This article has not been copyedited and formatted. The final version may differ from this version.

Running Title: "Microsomal vs Mitochondrial CYP1A1-Mediated Functions"

Pages of Text = 20

Tables = 1

Figures = 6

References = 53

Words in **Abstract** = 243

Words in **Introduction** = 407

Words in **Discussion** = 1871

Abbreviations used:

AHR, aryl hydrocarbon receptor**;** ALT, alanine aminotransferase**;** AST, aspartate aminotransferase**;** BaP, benzo[*a*]pyrene**;** BNF, β-naphthoflavone**;** DTT, dithiothreitol; ER, endoplasmic reticulum**;** MT, mitochondrial**;** POR, NADPH-P450 oxidoreductase**;** PHB, prohibitin**;** GCLM, glutamate-cysteine ligase modifier subunit**;** SRP, signal-recognition particle**;** ERND, erythromycin *N*-demethylase**;** FDX1, ferredoxin-1 (previous name: "adrenodoxin")**;** FDXR, ferredoxin reductase**;** CYP1A1, full-length translated protein from the mouse *Cyp1a1* gene**;** mc1A1, microsomal (ER)-targeted CYP1A1 protein**;** mt1A1, mitochondrial (MT)-targeted CYP1A1 protein**;** *Cyp1a1(+/+)* or *WT 1A1*, wild-type (C57BL/6J) mouse**;** *Cyp1a1(-/-)* or *KO 1A1*, mouse line having global knockout of the *Cyp1a1* gene**;** *Cyp1a1(mc/mc)* or *mc1A1*, line carrying ER-targeted CYP1A1 protein**;** *Cyp1a1(mtp/mtp)* or *mtp1A1*, line carrying MT-targeted CYP1A1 protein via proteolysis**;** *Cyp1a1(mtt/mtt)* or *mtt1A1*, line carrying MT-targeted CYP1A1 protein via truncation**;** TCDD or dioxin, 2,3,7,8-tetrachlorodibenzo-*p*-dioxin**;** MAD-PAGE, mixed-alcohol-detergent in polyacrylamide gel electrophoresis**;** SDS-PAGE, sodium dodecylsulfate in polyacrylamide gel electrophoresis**;** PKC, protein kinase-C

Molecular Pharmacology Fast Forward. Published on December 1, 2008 as DOI: 10.1124/mol.108.051888
This article has not been copyedited and formatted. The final version may differ from this version.

Abstract

Historically CYP1A1 protein is known to be located in the endoplasmic reticulum (**ER**; microsomes). More recently, CYP1A1 was shown to be targeted to the inner mitochondrial membrane**;** mitochondrial import is dependent on NH_2-terminal processing that exposes a cryptic targeting signal. Intriguingly, microsomal and mitochondrial CYP1A1 enzymes exhibit different substrate specificities, electron donors, and inducer properties. To understand the physiological functions of microsomal versus mitochondrial CYP1A1, we have generated three knock-in lines by altering the CYP1A1 NH_2-terminus. *Cyp1a1(mtt/mtt)* mice encode an NH_2-terminal 31-amino acid-**t**runcated protein, deleting the ER-targeting signal and exposing the cryptic **mi**t**o**chondrial-targeting signal. *Cyp1a1(mtp/mtp)* mice encode a protein carrying Leu7Asn and Leu17Asn mutations**;** this mutant lacks the signal recognition particle (**SRP**)-binding site and subsequent ER-targeting, but requires **p**roteolysis by a cytosolic peptidase for **mi**t**o**chondrial import. *Cyp1a1(mc/mc)* mice encode a **mi**c**r**osomal protein having Arg34Asp and Lys39Ile mutations which abolish the mitochondrial targeting signal. Following dioxin or β-naphthoflavone treatment of these mouse lines, the CYP1A1 protein was shown to be located in mitochondria of the *Cyp1a1(mtp/mtp)* and *Cyp1a1(mtt/mtt)* lines and in microsomes of the *Cyp1a1(mc/mc)* line. To test for differences in function, we compared the response to dietary benzo[*a*]pyrene (**BaP**). After 18 days of daily oral BaP, wild-type and *Cyp1a1(mc/mc)* mice were completely protected, whereas *Cyp1a1(-/-)* and *Cyp1a1(mtp/mtp)* mice showed striking toxicity and compensatory up-regulation of CYP1A2 and CYP1B1 mRNA in several tissues. Our data support the likelihood that it is the microsomal rather than mitochondrial CYP1A1 enzyme that protects against oral BaP toxicity.

Molecular Pharmacology Fast Forward. Published on December 1, 2008 as DOI: 10.1124/mol.108.051888
This article has not been copyedited and formatted. The final version may differ from this version.

Introduction

The cytochrome P450 monooxygenase superfamily includes 57 and 102 genes in the human and mouse genomes, respectively (Nelson et al., 2004). The *CYP1* family is one of 18 mammalian CYP families and contains three highly conserved members**:** *CYP1A1*, *CYP1A2* and *CYP1B1*. The basal and inducible expression of these three genes is regulated by the aryl hydrocarbon receptor (**AHR**) (Nebert et al., 2004;Puga et al., 2005;Hankinson, 2005;Nebert and Dalton, 2006;Kawajiri and Fujii-Kuriyama, 2007).

Historically CYP1A1 has been regarded as located only in the endoplasmic reticulum (**ER**), until a mitochondrial (**MT**) CYP1A1 was characterized in liver of rats pretreated with β-naphthoflavone (**BNF**) (Niranjan et al., 1985;Raza and Avadhani, 1988). Further investigations revealed that ER- versus MT-targeting of the CYP1A1 protein is determined by NH_2-terminal signal sequences. Depending on the tissue, animal's age and inducer pretreatment, varying amounts (from 5% to >50%) of CYP1A1 are directed to the MT inner-membrane by means of cryptic MT-targeting signals**;** a cytosolic peptidase-mediated proteolysis can result in either of two truncated isoforms of mitochondrial CYP1A1 (**mt1A1**)—one having the first four (rats) or eight (mice), the other having the first 32 (rats and mice), amino acids removed from the NH_2-terminus {119, 171}. In contrast to the NADPH-P450 oxidoreductase (**POR**)-mediated microsomal CYP1A1 (**mc1A1**) activity, mt1A1 activity depends on FDX1 (ferredoxin-1; previous name adrenodoxin) and FDXR (ferredoxin-1 reductase)**;** this distinction in the electron-donor complex might explain substrate-specificity differences seen between the mc1A1 and mt1A1 enzymes (Anandatheerthavarada et al., 1999).

Substrates for CYP1A1 include both endogenous compounds and exogenous chemicals (Nebert and Russell, 2002). Many studies have shown that CYP1A1 metabolism plays a major role in detoxication of foreign chemicals as well as metabolic activation leading to oxidative damage, birth

Molecular Pharmacology Fast Forward. Published on December 1, 2008 as DOI: 10.1124/mol.108.051888
This article has not been copyedited and formatted. The final version may differ from this version.

defects, DNA adduct formation, mutagenesis, and carcinogenesis (Nebert, 1989;Park et al., 1996;Nebert et al., 2000b;Nebert et al., 2004;Wells et al., 2005;Nebert and Dalton, 2006;Chung et al., 2007). It is tempting to speculate that mc1A1 metabolism might be predominantly involved in some of these processes whereas mt1A1 metabolism might be more important in others. To test these hypotheses, we have generated three knock-in mouse lines by targeted alteration of the *Cyp1a1* gene, such that the CYP1A1 protein is expected to be trafficked either to the ER (microsomes) or to the mitochondria. The present report describes the successful creation and characterization of these lines and then tests for functional differences, using the oral BaP paradigm previously described (Uno et al., 2004;Uno et al., 2006).

MATERIALS AND METHODS

Chemicals. Benzo[*a*]pyrene (**BaP**) and β-naphthoflavone (**BNF**) were purchased from Sigma-Aldrich (St. Louis, MO). 2,3,7,8-Tetrachlorodibenzo-*p*-dioxin (**TCDD**; dioxin) was purchased from Accustandard, Inc. (New Haven, CT). Ferredoxin (**FDX1**) and ferredoxin reductase (**FDXR**) were purified from bovine adrenal mitochondria, as described (Foster and Wilson, 1975;Raza and Avadhani, 1988). Erythromycin and SKF-525A were purchased from Sigma Chemical Company. All other chemicals and reagents were obtained from either Aldrich Chemical Co. (Milwaukee, WI) or Sigma-Aldrich at the highest available grades. Rabbit anti-human CYP1A1/CYP1A2 (**α-1A1/1A2**) polyclonal antibody was purchased from BD Gentest (Woburn, MA). Anti-NADPH-P450 oxidoreductase (**α-POR**) and anti-prohibitin (**α-PHB**) were bought from Abcam (Cambridge, MA). The polyclonal antibody to bovine ferredoxin (**α-FDX1**) was raised in the BALB/cJ mouse (Anandatheerthavarada et al., 1997). A polyclonal antibody to mouse glutamate-cysteine ligase modifier subunit (**α-GCLM**) was generated in the chicken (Chen et al., 2007).

Generation of Targeting Constructs. A 352-bp *Cyp1a1* genomic gene fragment, excised by *Sac*I and *Apa*I from the 7.58-kb *Eag*I-*Eco*RV fragment (Dalton et al., 2000), was cloned into the pBluescript II KS$^-$

Molecular Pharmacology Fast Forward. Published on December 1, 2008 as DOI: 10.1124/mol.108.051888
This article has not been copyedited and formatted. The final version may differ from this version.

vector (**Fig. 1A**) to use as template DNA for site-directed mutagenesis. Using QuikChange® site-directed mutagenesis kits (Stratagene, La Jolla, CA), we mutated the *Sac*I-*Apa*I fragment at codons 7 & 17, or we mutated codons 34 & 39**;** alternatively, we made a 93-bp deletion resulting in the removal of 31 NH_2-terminal amino acids (**Fig. 1B**). Subsequently, these were cloned back into the pBluescript II KS^- vector that carried the *Cyp1a1* 7.58-kb *Eag*I-*Eco*RV fragment—to generate the three *Cyp1a1* mutant allele-targeting vectors (**Figs. 1A** & **1B**). A *NEO* mini-cassette (Mansour et al., 1988), containing an extra *EcoR*V site flanked by direct-repeat *loxP* sites (Gu et al., 1994), was inserted into the *Cyp1a1* intron 1 unique *Sac*I site. This was followed by cloning of the HSV-*TK* gene (Capecchi, 1989), flanked by *Xho*I and *Sac*II at the 3' end of the *Eag*I-*Eco*RV fragment, to make the targeting constructs (**Fig. 1A**, *2nd line*). All constructs were linearized by digestion with *Sac*II, prior to microinjection into 129/SvJ mouse embryonic stem (**ES**) cells by the Mouse Transgenesis Core in the Center for Environmental Genetics, University of Cincinnati.

Southern blot hybridization. DNA, extracted from ES cell colonies followed sequentially by *EcoR*V digestion, was examined by Southern blot on Nytran SuperCharge membranes (Schleicher & Schuell; Keene, NH) via capillary-transfer. A 792-bp region, which is 53 bp upstream (outside the targeting region) from the 5' end of the *Eag*I-*Eco*RV fragment, was used as template DNA for the probe generated by PCR (**Fig. 1A**, *3rd line*). Primers used (flanking the 792-bp probe for Southern blot) were**:** for forward 5'-ACAGGGGAGGGCAGGTGAAGGT-3' and reverse 5'-TCACCTCTAAGGGTCACCTTAG-3'. ^{32}P-labeled random-primed DNA probes (2 x 10^6 cpm/ml) were hybridized overnight with *EcoR*V-digested genomic DNA blotted on the membranes—following prehybridization at 65°C for 4 h in 6X SSC, 10X Denhardt's, and 1% sodium dodecylsulfate (**SDS**). Membranes were washed in 1X SSC + 0.1% SDS at 65°C for 1 h**;** then washed in 0.2X SSC + 0.1% SDS**;** and finally washed in 0.1X SSC + 0.1% SDS at 65°C for 20 min twice, followed by a 48-h exposure to Kodak X-OMAT film (Rochester, NY).

Generation of *Cyp1a1(mc/mc), Cyp1a1(mtp/mtp), Cyp1a1(mtt/mtt)* mouse lines. Targeted ES cells (agouti) were microinjected into the blastocoele cavity of C57BL/6J embryos (non-agouti), and blastocysts were transferred into pseudopregnant CD-1 foster dams (Li et al., 1994). Identification of chimeric pups was determined by the presence of agouti coat color at 10 days of age. Male chimeric mice were then bred to

Molecular Pharmacology Fast Forward. Published on December 1, 2008 as DOI: 10.1124/mol.108.051888
This article has not been copyedited and formatted. The final version may differ from this version.

C57BL/6J females, and agouti-colored offspring were screened by PCR for presence of the *NEO* gene, denoting germ-line transmission of the targeted *Cyp1a1* alleles (**Fig. 1A**, *3rd line*). Heterozygotes carrying the *lox*P-flanked *NEO* gene were then bred with mice carrying bacterial *Cre* driven by the chicken β-actin promoter (Araki et al., 1995) to remove the *NEO* gene cassette**;** this resulted in the final three targeted *Cyp1a1* alleles without *NEO* (**Fig. 1A**, *bottom line*). Breeding of heterozygotes generated homozygosity of the targeted alleles, which were genotyped by taking advantage of the extra 34-bp *loxP* site.

Animals. The *Cyp1a1(mc/mc)*, *Cyp1a1(mtp/mtp)*, *Cyp1a1(mtt/mtt)* and *Cyp1a1(-/-)* mouse lines were backcrossed into C57BL/6J for eight generations**;** this ensured that the knock-in genotypes reside in a genetic background that is >99.8% C57BL/6J (Nebert et al., 2000a). Age-matched C57BL/6J mice, purchased from The Jackson Laboratory (Bar Harbor, ME), could thus be used as *Cyp1a1(+/+)* wild-type (*WT 1A1*) controls. The *Cyp1a1(-/-)* knockout mouse line (Dalton et al., 2000) was used as the CYP1A1-null control. All animal experiments were approved by, and conducted in accordance with, the National Institutes of Health (NIH) standards for the care and use of experimental animals and the University Cincinnati Medical Center Institutional Animal Care & Use Committee (IACUC).

Biohazard Precaution. BaP and TCDD are regarded as highly toxic and probable human carcinogens. All personnel were instructed in safe handling procedures. Lab coats, gloves, and masks were worn at all times, and contaminated materials were collected separately for disposal by the Hazardous Waste Unit or by independent contractors. BaP- and TCDD-treated mice were housed separately, and their carcasses regarded as contaminated biological materials.

Pretreatment. TCDD (5 μg/ml) and BNF (8 mg/ml) were dissolved in corn oil. *Cyp1a1(+/+)*, *Cyp1a1(mc/mc)*, *Cyp1a1(mtp/mtp)*, *Cyp1a1(mtt/mtt)* and *Cyp1a1(-/-)* mice were given intraperitoneal TCDD (15 μg/kg for 3 consecutive days) or BNF (80 mg/kg for 10 consecutive days), as described (Boopathi et al., 2000;Uno et al., 2004). At 10 days after initiating TCDD or BNF treatment, four tissues (kidney, lung, small intestine, liver) were collected. These regimens allow optimal accumulation of the CYP1A1 protein in mitochondria (Boopathi et al., 2000;Genter et al., 2006).

Molecular Pharmacology Fast Forward. Published on December 1, 2008 as DOI: 10.1124/mol.108.051888
This article has not been copyedited and formatted. The final version may differ from this version.

For the oral BaP experiments with these new lines, no differences in weight gain or immunosuppression between males and females were found after 5 or 15 days on dietary BaP**;** thus, males only were chosen for further studies. BaP, given in corn oil-soaked food, was administered to 6-week-old *Cyp1a1(+/+)*, *Cyp1a1(mc/mc)*, *Cyp1a1(mtp/mtp)* and *Cyp1a1(-/-)* male mice. The rodent food (Harlan Teklad, Madison, WI) was soaked at least 24 h in BaP-containing corn oil (10 mg/ml) before being offered to the mice. By knowing the weight of the food ingested daily by a 20-g mouse and by using [^{3}H]benzo[*a*]pyrene in early experiments (Robinson et al., 1975), we estimated the daily oral BaP dose to be ~125 mg/kg/day. To start day 1 of the experiment, after an overnight fast mice were presented with the BaP-laced food**;** control mice received food soaked in corn oil alone. Mice eagerly eat corn oil-soaked food. The oral BaP experiments were concluded on day 18, which is when some mouse lines exhibit weight loss but no animals are overtly ill (Uno et al., 2004;Uno et al., 2006). All tissues were harvested between 9:00 and 10:00 am to exclude any circadian rhythm effects.

Reverse Transcription. Total RNA was isolated (liver, kidney, lung, small intestine, spleen; N= 4 mice per group) using the TRI Reagent total RNA isolation reagent (MRC; Cincinnati, OH). Total RNA (1 μg) was added to a final reaction solution of 13 μL containing oligo(dT)$_{20}$ (3.8 μM) and dNTP (0.77 mM). Reactions were incubated at 65°C for 5 min and chilled on ice for 2 min. To the reaction mixture was added 7 μL of a solution containing 200 units of SuperScript III and 5 μM dithiothreitol (Invitrogen, Carlsbad, CA). Reactions were incubated at 50°C for 50 min, followed by 85°C for 10 min (to inactivate the reverse transcriptase). The cDNA samples were stored at –80°C until further study.

Quantitative real-time polymerase-chain reaction (qRT-PCR). Primers used for detecting mouse mRNA were**:** for CYP1A1, forward (f) 5'-CCTCATGTACCTGGTAACCA-3' and reverse (r) 5'-AAGGATGAATGCCGGAAGGT-3'**;** for CYP1A2, (f) 5'-AAGACAATGGCGGTCTCATC-3' and (r) 5'-GACGGTCAGAAAGCCGTGGT-3'**;** for CYP1B1, (f) 5'-ACATCCCCAAGAATACGGTC-3' and (r) 5'-TAGACAGTTCCTCACCGATG-3'**;** for β-actin, (f) 5'-CATCCGTAAAGACCTCTATGCC-3' and (r) 5'-ACGCAGCTCAGTAACAGTCC-3'. The qRT-PCR was performed with the ABI Prism 7000 Sequence

Molecular Pharmacology Fast Forward. Published on December 1, 2008 as DOI: 10.1124/mol.108.051888
This article has not been copyedited and formatted. The final version may differ from this version.

Detection System (Applied Biosystems), using iQ™ SYBR Green Supermix (BIO-RAD, Hercules, CA). Each sample was normalized to β-actin mRNA.

Western immunoblot analysis. Kidney, small intestine and liver were chopped finely and homogenized on ice in 50 mM potassium phosphate buffer containing 0.1 mM EDTA and 1.15% KCl. Small pieces of lung were homogenized in H-medium, as described (Bhagwat et al., 1999). The homogenates were centrifuged at 500 × g for 15 min**;** supernatant fractions were centrifuged at 1000 × g for another 15 min, followed by centrifugation of the supernatant at 10,000 × g for 15 min. The pellets were resuspended and repeatedly centrifuged at 10,000 × g five more times, to acquire relatively pure mitochondrial fractions. The resulting supernatant fractions were centrifuged at 18,000 × g for 30 min, followed by centrifugation of the resulting supernatants at 100,000 × g for 60 min to obtain the microsomal fractions. The pellets were resuspended, quantified, and subjected to electrophoresis on a 12% SDS or mixed-alcohol-detergent (**MAD**) (Brown, 1988) polyacrylamide mini-gel under denaturing conditions. Proteins were then transferred to nitrocellulose membranes for immunoblotting. The membrane was blocked with 3% bovine serum albumin in **TTBS** (1.5 M sodium chloride, 0.1 M Tris, pH 7.4, containing 0.1% Tween 20) followed by incubation overnight at 4°C with α-1A1/1A2, α-POR, α-PHB, or α-GCLM. After triplicate washes in PBST, the membranes were incubated with horseradish peroxidase-conjugated secondary antibody (Santa Cruz Biotechnology, Santa Cruz, CA; 1:10,000) for 60 min. After triplicate washes, protein bands were visualized, using enhanced chemiluminescence (ECL, Amersham; Piscataway, NJ).

Enzyme assays. BaP hydroxylase activity was assayed by the standard spectrophotofluorometric method (Nebert and Gelboin, 1968)**:** determining the rate of formation of hydroxylated products of BaP (pmol/min/mg protein). Erythromycin N-demethylase (**ERND**) activity was assayed spectrophotometrically (Anandatheerthavarada et al., 1999;Boopathi et al., 2000), by following the rate of HCHO formation (nmol/min/mg protein).

Detection of BaP in blood. BaP levels in whole blood were quantified by modification of previously described methods (Garcia-Falcon et al., 1996;Kim et al., 2000). Whole blood (30 μL) was extracted three

Molecular Pharmacology Fast Forward. Published on December 1, 2008 as DOI: 10.1124/mol.108.051888
This article has not been copyedited and formatted. The final version may differ from this version.

times with ethyl acetate/acetone mixture (2:1, v:v). The organic extracts were pooled and dried under argon, and the residue resuspended in 250 μL of acetonitrile. An aliquot (100 μL) was injected onto a Nova-Pak C_{18} reverse-phase column (4-μm, 150 x 3.9 mm i.d.; Waters Associates; Boston, MA). HPLC analysis was conducted on a Waters™ Model 600 solvent controller, equipped with a fluorescence detector (F-2000, Hitachi). Isocratic separation was performed using an acetonitrile:water (85:15, v:v) mobile phase at a flow-rate of 1 ml/min. Excitation and emission wavelengths were 294 and 404 nm, respectively. BaP concentrations in blood were calculated by comparing the peaks of samples with those of control blood that had been spiked with different known concentrations of BaP. The calibration curve for BaP showed excellent linearity (correlation coefficient r >0.998); four major and several minor BaP metabolites were found to run far ahead of BaP on the column, and thus did not interfere. The detection limit (defined as 3 times the signal-to-noise ratio) was 0.05 pg/μL, and the limit of BaP quantification was determined to be 0.20 pg/μL. The intra-day and inter-day precision of repeated analyses (N=4) gave us coefficients of variation of <12%.

Plasma Enzymes. Peripheral blood was collected following 18 days of dietary BaP. Plasma was isolated from centrifuged whole blood for measuring alanine aminotransferase (**ALT**) and aspartate aminotransferase (**AST**) activities, using kits purchased from Sigma-Aldrich.

Statistical Analysis. Statistics were performed using SigmaStat Statistical Analysis software (SPSS Inc., Chicago, IL). Group means were compared by one-way ANOVA, followed by Student's *t*-test for pairwise comparison-of-means. All data were normally distributed and are reported as the means ± S.E.M. *P*-values of <0.05 were considered statistically significant.

RESULTS

Generation of Knock-In Mouse Lines. In previous studies (Addya et al., 1997), ER- versus MT-targeting of rat and mouse CYP1A1 protein was reported to be due to NH_2-terminal chimeric signal sequences in the segment from residues 1 to 44: the amino-acid stretch from 1 to 30 provides signals for ER membrane insertion and stop transfer; amino acids 33 to 44 provide MT-targeting signals.

Molecular Pharmacology Fast Forward. Published on December 1, 2008 as DOI: 10.1124/mol.108.051888
This article has not been copyedited and formatted. The final version may differ from this version.

Mouse Leu7 and Leu17 are critical for SRP-binding (and thus ER-targeting), whereas positively-charged Arg34 and Lys39 function critically for MT-targeting.

Based on this knowledge, by site-directed mutagenesis we made genetic alterations in the *Cyp1a1* wild-type gene (**Fig. 1**). Mutations at codon-34 (AGA→GAC) and codon-39 (AAA→ATA), to produce Arg34Asp and Lys39Ilu, respectively, should target the CYP1A1 protein only to the ER**;** this "**m**i**c**rosomal-only CYP1A1 line" is called *mc1A1* (Fig. 1B, *2nd line*). Removal of 93 bp (encoding residues 2-32) replaces Ala32 with methionine, and this truncated CYP1A1 protein should be targeted only to the mitochondria because the entire ER-insertion domain is missing**;** this "**m**i**t**ochondrial-only **t**runcated CYP1A1 line" is called *mtt1A1* (**Fig. 1B**, *3rd line*). Mutations at codon-7 (CTT→AAT) and codon-17 (CTC→AAC), to produce Leu7Asn and Leu17Asn, respectively, should target the CYP1A1 protein exclusively to mitochondria, but only after cytosolic proteolysis**;** this "**m**i**t**ochondrial-only **p**roteolysis CYP1A1 line" is called *mtp1A1* (**Fig. 1B**, *last line*).

These organelle-specific variations were cloned into exon 2 of the targeting constructs (**Fig. 1A**), and then the linearized constructs were independently electroporated into 129/SvJ mouse embryonic stem cells for homologous recombination with the genomic *Cyp1a1* gene. The occurrence of homologous recombination between targeting constructs and the genomic *Cyp1a1* gene was confirmed by PCR, followed by Southern blot hybridization. By use of a primer inside the *NEO* cassette and a primer 20 bp downstream of the targeting constructs, ~10% of ES cell colonies showed positive targeting by PCR screening (data not shown). Further testing by Southern blot hybridization (**Fig. 1C**) by using a probe 53 bp upstream of the targeting constructs (**Fig. 1A**, *3rd line*), we verified the proper incorporation of organelle-specific mutations into the *Cyp1a1* locus. Male chimeric mice having partial or complete agouti coat-color were then bred to C57BL/6J females. Mice with agouti coats and carrying the *NEO* gene, which represents germ-line transmission of the targeted allele, were

Molecular Pharmacology Fast Forward. Published on December 1, 2008 as DOI: 10.1124/mol.108.051888
This article has not been copyedited and formatted. The final version may differ from this version.

crossed with mice carrying the bacterial *Cre* gene driven by the chicken β-actin promoter (Araki et al., 1995). This removes the *NEO* gene mini-cassette from the mouse genome via Cre-*loxP*-mediated recombination, giving the final targeted *Cyp1a1* allele carrying an extra *loxP* site of 34 bp in intron 1 (**Fig. 1A**, *bottom line*). Mice homozygous for the targeted alleles, confirmed by genotyping for the extra *loxP* site (**Fig. 1D**)—are viable, fertile, and display no overt phenotype.

CYP1A mRNA Expression Levels in Knock-In Lines. TCDD and BNF are known AHR ligands, causing CYP1A1 induction and mitochondrial import (Boopathi et al., 2000;Uno et al., 2004;Uno et al., 2006). Following TCDD pretreatment (**Fig. 2A**), qRT-PCR analysis displayed no differences in CYP1A1 mRNA levels among each of the individual organs—liver, kidney, lung or small intestine—when we compared *mc1A1*, *mtt1A1* and *mtp1A1* mice with wild-type mice**;** exceptions included more highly induced CYP1A1 mRNA in kidney and in small intestine of *mtt1A1* and *mtp1A1* mice. In contrast and as expected, no CYP1A1 mRNA was detected in the *Cyp1a1(-/-)* knockout mouse. Following BNF pretreatment (**Fig. 2B**), qRT-PCR analysis displayed significantly higher amounts (5- to 8-fold) of CYP1A1 mRNA only in liver and kidney of *mc1A1* than that of wild-type mice. Again, no CYP1A1 mRNA was detected in the *KO 1A1* knockout mouse.

Fig. 2A shows that the basal CYP1A2 mRNA level in small intestine was negligible, but TCDD-induced CYP1A2 mRNA was statistically significantly elevated in *mtt1A1* (3.2-fold), *mtp1A1* (1.3-fold), and *KO 1A1* (7.4-fold) mice—compared with that in TCDD-treated *WT 1A1* and *mc1A1* mice**;** these intriguing data suggest that absence of the mc1A1 but not the mt1A1 protein (or presence of the mt1A1 but not the mc1A1 protein) in small intestine might cause up-regulate the *Cyp1a2* gene by TCDD (Uno et al., 2008). **Fig. 2B** illustrates no differences in basal or in BNF-induced hepatic CYP1A2 mRNA levels among the wild-type, *mc1A1*, *mtt1A1*, or *mtp1A1* or *KO 1A1* mice. TCDD-induced CYP1A2 mRNA levels are negligible in kidney and lung, except slightly elevated in *KO 1A1*

Molecular Pharmacology Fast Forward. Published on December 1, 2008 as DOI: 10.1124/mol.108.051888
This article has not been copyedited and formatted. The final version may differ from this version.

(**Figs. 2A & 2B**).

Subcellular Distribution of CYP1A1 Protein. Following TCDD or BNF pretreatment (**Fig. 3**), organelle-targeting of the CYP1A1 protein was examined in *WT 1A1*, *mc1A1*, *mtt1A1*, and *mtp1A1* mice. Microsomal and mitochondrial proteins were resolved by SDS-PAGE or MAD-PAGE (Brown, 1988), the latter rendering a superior separation of the 56-kDa CYP1A1 from the 54.5-kDa CYP1A2 protein. Subcellular distribution of the CYP1A1 protein was compared by Western immunoblot using microsomal POR, mitochondrial PHB, and cytosolic GCLM as subcellular-specific markers. Distribution of the CYP1A1 protein (**Fig. 3**) was consistent with the CYP1A1 mRNA levels in the various tissues (**Fig. 2**). The CYP1A1 protein in kidney (**Fig. 3A**, *upper left*) was found**:** in TCDD-treated but not untreated *WT 1A1* mitochondria and microsomes, in TCDD-treated *mc1A1* microsomes but not mitochondria, predominantly in TCDD-treated *mtt1A1* mitochondria more so than microsomes, and predominantly in TCDD-treated *mtp1A1* mitochondria more so than microsomes. The same pattern was seen in lung (**Fig. 3A**, *upper right*) and small intestine after TCDD treatment (**Fig. 3A**, *lower left*) and lung after BNF treatment (**Fig. 3A**, *lower right*).

In TCDD-treated *mtt1A1* and *mtp1A1* mice, trace amounts of CYP1A1 protein were detectable in the ER fractions of lung (**Fig. 3A**, *upper right*) and especially of liver (not shown). The liver contains so much ER that we always faced some degree of contamination of mitochondrial fragments by microsomes, and this was confirmed using the specific organelle markers. However, when specific subcellular markers are included—POR for microsomes, PHB for mitochondria, and GCLM for cytosol—no detectable contamination was seen on the Western blots (**Fig. 3**). In our experience, kidney and lung clearly provided more robust separations of mitochondria from microsomes (and vice versa) than small intestine, and especially more robust than liver.

CYP1A2 protein cannot be detected on Western immunoblots from kidney or lung, and cannot be

Molecular Pharmacology Fast Forward. Published on December 1, 2008 as DOI: 10.1124/mol.108.051888
This article has not been copyedited and formatted. The final version may differ from this version.

detected in small intestine following TCDD pretreatment [whereas CYP1A2 protein is detectable following oral BaP treatment (Uno et al., 2008)]. On the other hand, CYP1A2 protein levels are very high in the liver of control as well as TCDD- or BNF-pretreated mice. These are the reasons why in **Fig. 3** we chose to show immunoblots probed by α-1A1/1A2 from kidney, lung and intestine of TCDD-treated mice and from lung of BNF-treated mice.

Importantly, no CYP1A1 protein was detected in any of the cytosolic fractions (**Fig. 3B**), indicating that those CYP1A1 proteins without microsomal targeting signals do not inherently accumulate in cytoplasm. In summary, the data in **Fig. 3** confirm that the CYP1A1 protein has been successfully targeted in the tissues examined, and into the expected subcellular compartment**:** mc1A1 protein in the *mc1A1* line, and mt1A1 protein in the *mtt1A1* and *mtp1A1* lines.

Enzyme Activities in the Cyp1a1 Knock-In Lines. Differences in substrate specificities for mt1A1 versus mc1A1 in metabolizing particular drugs, such as erythromycin and psychotropic drugs including morphine (Anandatheerthavarada et al., 1999;Dasari et al., 2006), have been reported. Because drug metabolism is far more robust in liver than nonhepatic tissues, we compared ERND and BaP hydroxylase activities in hepatic mitochondria versus microsomes. Mitochondrial fractions in the BNF-treated *mtt1A1* and *mtp1A1* lines displayed significantly higher ERND activity than that in *WT 1A1* or *mc1A1* mice (**Fig. 4A**, *upper panel*)**;** in microsomal fractions, no differences in ERND activity were seen among the groups of BNF-treated mice (**Fig. 4A**, *lower panel*)—although ERND was induced by BNF to levels ~1.5-fold higher than basal ERND activity.

Microsomal CYP1A1, in the presence of POR added in vitro, is known to exhibit virtually no ERND activity, whereas mt1A1 in the presence of added FDX1 and FDXR shows very high ERND activity (Anandatheerthavarada et al., 1997;Anandatheerthavarada et al., 1999;Boopathi et al., 2000). BNF-induced ERND thus represents the mt1A1 protein, whereas mitochondrial basal ERND activity

Molecular Pharmacology Fast Forward. Published on December 1, 2008 as DOI: 10.1124/mol.108.051888
This article has not been copyedited and formatted. The final version may differ from this version.

may reflect either CYP1A2 or CYP2D, both of which exist in mitochondria (Boopathi et al., 2000). In all likelihood, microsomal basal and BNF-inducible ERND activities reflect one or more of the CYP3A enzymes (Xu et al., 2006)**;** this most likely explains why we see nearly equal ERND activity in microsomes of all the BNF-treated mouse lines.

Fig. 4A (*upper panel*) shows that, in mitochondria of BNF-treated animals, an antibody to FDX1 inhibited ERND activity ~70% in *mtt1A1* and ~45% in *mtp1A1* mice, compared with ~30% in *WT 1A1* mice and negligible amounts in *mc1A1* mice. These findings confirm further the mt1A1 protein is the principal contributor to mitochondrial ERND activity in the *mtt1A1* and *mtp1A1* lines.

Fig. 4A (*upper* and *lower panels*) illustrates that ERND activity can be completely inhibited by 2-diethylaminoethyl-2,2-diphenylvalerate hydrochloride (**SKF-525A**) in both mitochondria and microsomes of all mice. These data confirm that P450 monooxygenases are responsible for virtually all of the detectable ERND activity in these assays.

Hepatic microsomes from BNF-treated *WT 1A1* and *mc1A1* mice (**Fig. 4B**, *top panel*) showed a ~3.7- and 3.5-fold induction of BaP hydroxylase activity, respectively, compared with untreated *WT 1A1* mice**;** this finding confirms that BNF-induced BaP hydroxylase in the *mc1A1* line indeed reflects mc1A1 protein. BNF-treated *KO 1A1* mice showed no significant increases in BaP hydroxylase activity over that seen in the untreated wild-type mouse**;** these data are consistent with numerous previous reports describing the *Cyp1a1(-/-)* mouse treated with various CYP1A1 inducers (Dalton et al., 2000;Uno et al., 2001;Uno et al., 2004;Jiang et al., 2005;Derkenne et al., 2005;Cheung et al., 2005;Uno et al., 2006;Genter et al., 2006;Ma et al., 2007;Dragin et al., 2007;Uno et al., 2008). BaP hydroxylase activity which exists in liver of untreated mice is known to reflect a CYP2C enzyme {170}. On the other hand, hepatic microsomes from BNF-treated *mtp1A1* mice produced ~1.6-fold greater induced BaP hydroxylase activity, compared with untreated *WT 1A1* mice**;** we believe this

Molecular Pharmacology Fast Forward. Published on December 1, 2008 as DOI: 10.1124/mol.108.051888
This article has not been copyedited and formatted. The final version may differ from this version.

reflects the degree of contamination of liver mitochondria in the microsomal fractions.

The differences in microsomal BaP hydroxylase activity are much more easily visualized in kidney and lung than in liver for two reasons**:** [a] basal BaP metabolism is negligible in untreated *WT 1A1* mice**;** [b] due to the abundance of microsomes in liver and therefore contamination of the mitochondrial fraction with microsomes (and vice versa), separation of the two organelles is much less problematic in kidney and lung. Hence, relative to the untreated *WT 1A1* (**Fig. 4B**, *middle panel*), a 50- to 60-fold induction of kidney BaP hydroxylase activity was seen in BNF-treated *WT 1A1* and *mc1A1* mice, compared with a ~10-fold induction of enzyme activity in BNF-treated *mtp1A1* mice. A ~40- and ~20-fold induction of lung BaP hydroxylase activity (**Fig. 4B**, *lower panel*) is seen in BNF-treated *WT 1A1* and *mc1A1* mice, respectively, compared with a no detectable induction of enzyme activity in BNF-treated *mtp1A1* mice. These differences in microsomal BaP hydroxylase activity, comparing BNF-treated *WT1A1* with the *mc1A1* and *mtp1A1* lines, are therefore consistent with the qRT-PCR (**Fig. 2B**) and Western immunoblot data (**Fig. 3A**). In the *Cyp1a1(-/-)* mouse, a compensatory up-regulation of CYP1B1 has previously been noted (Uno et al., 2006;Uno et al., 2008), which would explain the small increases in BaP hydroxylase activity observed in liver, kidney and especially lung.

Proof-of-Principle Experiments in mc1A1 versus mt1A1 Following Oral BaP. We wanted to show a clinical difference between mc1A1- and mt1A1-containing mice. Previous studies (Raza and Avadhani, 1988) have shown that the mt1A1 protein is ~10% as efficient as the mc1A1 protein in BaP metabolism in vitro. Previous oral BaP studies have shown that intestinal (and perhaps hepatic) CYP1A1 functions primarily in the process of detoxication, to protect the mouse against oral BaP-induced immunosuppression (Uno et al., 2004;Uno et al., 2006). We therefore evaluated the role of mc1A1 versus mt1A1 in animals receiving oral BaP. Because of the numbers of mice needed and

Molecular Pharmacology Fast Forward. Published on December 1, 2008 as DOI: 10.1124/mol.108.051888
This article has not been copyedited and formatted. The final version may differ from this version.

expenses, we completed all studies with only *mtp1A1* mice, although preliminary data with *mtt1A1* mice (not shown) were very similar.

After 5 days of continuously administered oral BaP, whole blood BaP levels in *mc1A1* mice were not different from that of *WT 1A1* mice**;** by contrast, BaP levels were ~11-fold and ~25-fold higher in *mtp1A1* and *KO 1A1*, respectively, than in *WT 1A1* mice (**Fig. 5**). Thus, the *mtp1A1* line is more similar to the *Cyp1a1(-/-)* knockout line than the *mc1A1* line**;** these data support our hypothesis that, in the wild-type mouse, it is mc1A1 rather than mt1A1 that is responsible for detoxication of oral BaP.

The data in **Table 1** are consistent with previous studies (Uno et al., 2004;Uno et al., 2006). The *Cyp1a1(-/-)* knockout mouse treated with oral BaP for 18 days exhibits striking oral BaP-induced damage, including**:** [a] the wasting syndrome as seen by lowered body weight**;** [b] immunosuppression as shown by decreased spleen and thymus weight, lymphocytopenia, and bone marrow hypocellularity accompanied by a decreased ratio of lymphoid to myeloid series of cells**;** [c] anemia as revealed by decreased hematocrit and hemoglobin**;** [d] enhanced oxidative stress as evidenced by elevated methemoglobin**;** and [e] liver toxicity as depicted by increased liver weight and elevated plasma ALT and AST activities. These parameters are associated with mortality in *Cyp1a1(-/-)* mice that is seen after ~28 days of continuous oral BaP exposure (Uno et al., 2004;Uno et al., 2006).

At 125 mg/kg/day of oral BaP for 18 days, *WT 1A1* and *mc1A1* mice did not show any of these abnormalities (**Table 1**). On the other hand, *mtp1A1* mice displayed moderate degrees of toxicity in each of the above-mentioned parameters. The data in **Table 1** are thus consistent with the whole blood BaP levels in these lines (**Fig. 5**) and suggest that absence of the mc1A1 protein in the *mtp1A1* mouse leads to oral BaP-induced whole-body damage—albeit to a lesser extent, when compared with

Molecular Pharmacology Fast Forward. Published on December 1, 2008 as DOI: 10.1124/mol.108.051888
This article has not been copyedited and formatted. The final version may differ from this version.

that in the *Cyp1a1(-/-)* knockout mouse.

CYP1 mRNA Levels in Oral BaP-Treated Mice. In order to understand *Cyp1* expression in several organs following 18 days of oral BaP administration, we measured mRNA levels from all three *Cyp1* genes in small intestine, liver and spleen. CYP1A1 mRNA was not detectable in any of the three tissues from the *Cyp1a1(-/-)* mouse. Oral BaP-induced CYP1A1 mRNA levels (**Fig. 6**, *top row*) in small intestine were >2-fold higher in *mtp1A1* than in *mc1A1* or *WT 1A1*. In liver, CYP1A1 mRNA in *mtp1A1* was ~70-fold higher than that in *mc1A1*, and ~560-fold greater than that in *WT 1A1*. In spleen of oral BaP-treated mice, CYP1A1 mRNA concentrations were >10-fold higher in *mtp1A1* than in *mc1A1* or *WT 1A1*.

Oral BaP-induced CYP1A2 mRNA levels (**Fig. 6**, *middle row*) in small intestine were not different among the four oral BaP-treated groups examined**;** however, basal CYP1A2 mRNA concentrations were ~10-fold elevated in the untreated *KO 1A1* mouse—suggesting that complete absence of intestinal CYP1A1 causes a compensatory up-regulation of the basal CYP1A2 mRNA. This finding (in small intestine, but not in liver or spleen) is consistent with what had been found previously (Uno et al., 2006;Uno et al., 2008). In liver, oral BaP-induced CYP1A2 mRNA levels in *mtp1A1* and *KO 1A1* mice were >3-fold higher than that in *mc1A1*, and ~9-fold greater than that in *WT 1A1* mice. In spleen, oral BaP-induced CYP1A2 mRNA concentrations were ~7-fold higher in *KO 1A1* than in *mtp1A1*, which in turn were ~3-fold greater than that in *mc1A1* or *WT 1A1*.

Oral BaP-induced CYP1B1 mRNA levels (**Fig. 6**, *bottom row*) in intestine were >5-fold higher in *KO 1A1* than in *mtp1A1* mice, and CYP1B1 mRNA was ~12-fold greater in *mtp1A1* than that in *mc1A1* or *WT 1A1*. A compensatory up-regulation of basal CYP1B1 mRNA was observed in small intestine of both the *KO 1A1* and *mtp1A1* mice**;** this finding (seen in small intestine, but not in liver or spleen) is consistent with what had been reported previously (Uno et al., 2006;Uno et al., 2008). In

Molecular Pharmacology Fast Forward. Published on December 1, 2008 as DOI: 10.1124/mol.108.051888
This article has not been copyedited and formatted. The final version may differ from this version.

liver, oral BaP-induced CYP1B1 mRNA levels in the *KO 1A1* and *mtp1A1* mice were >700-fold and ~25-fold higher, respectively, than that in *mc1A1* or *WT 1A1* mice. In spleen, oral BaP-induced CYP1B1 mRNA concentrations in the *KO 1A1* and *mtp1A1* mice were ~7-fold and ~2-fold greater, respectively, than that in *mc1A1* or *WT 1A1* mice.

Our findings in the two knock-in lines (**Figs. 5 & 6**; **Table 1**) follow the pattern that the *mc1A1* line is more capable of detoxication of oral BaP than the *mtp1A1* line**:** BaP is cleared more readily from the *mc1A1* gastrointestinal tract (similar to what is seen in the wild-type GI tract), leading to lower BaP blood levels and less BaP inducer reaching the liver or spleen and, hence, lower CYP1 mRNA accumulation in the *mc1A1* than the *mtp1A1* line in these two organs.

DISCUSSION

For the past decade it has been appreciated that the mammalian CYP1A1 protein is located in both the ER and the inner membrane of mitochondria**;** relative amounts vary—depending on the species (rat, mouse or human), age, and the organ or tissue being studied (Raza and Avadhani, 1988;Addya et al., 1997;Anandatheerthavarada et al., 1997). Moreover, differences in inducer, as well as substrate and electron donor specificity, exist between mc1A1 and mt1A1 (Raza and Avadhani, 1988;Addya et al., 1997;Anandatheerthavarada et al., 1997). The obvious questions include**:** why have these two different subcellular CYP1A1 proteins evolved during the past 70 million years of the mammalian radiation, and what special critical life function(s) is(are) specific to one or the other?

It therefore seemed reasonable to genetically engineer mouse lines carrying either an exclusively ER-targeted or an exclusively MT-targeted CYP1A1 protein. Although the proposed feat had no 100% guarantee of success, the present study (**Figs. 1 & 3**) confirms that we have accomplished our aim. Given this success, a proof-of-principle experiment was then performed in order to show

Molecular Pharmacology Fast Forward. Published on December 1, 2008 as DOI: 10.1124/mol.108.051888
This article has not been copyedited and formatted. The final version may differ from this version.

differences in function by mc1A1 versus mt1A1 in the intact animal**;** this was done, by using the oral BaP paradigm previously studied in these laboratories, and we show (**Fig. 5**; **Table 1**) that the mc1A1 appears to be more important than the mt1A1 protein in the detoxication of oral BaP.

ER-Specificity of the Targeted CYP1A1 Protein. Following stringent centrifugation, it was rare to see microsomes contaminated by MT fractions (as judged by our finding no MT-specific marker PHB in microsomal fractions—especially TCDD-treated kidney, BNF-treated lung)**;** we therefore believe that the CYP1A1 protein detected in microsomes in *mc1A1* mice is indeed the microsomal form. By way of Western immunoblot analysis (**Fig. 3**), the ER-targeted mc1A1 protein appeared to be localized ~100% to the microsomes (and not mitochondria) in lung, kidney and small intestine from TCDD-induced *mc1A1* mice**;** these data indicate that our site-directed mutagenesis experiments, to efficiently block the MT-targeting signal (Fig. 1), were successful in preventing import of CYP1A1 protein into mitochondria.

In the liver from TCDD or BNF-treated *mc1A1* mice, however, there were always small but detectable amounts of anti-CYP1A1-reactive protein in mitochondrial fractions—whether isolated via repeated differential centrifugations or via digitonin-stripped mitoplasts (data not shown). Because there was always the concomitant presence of small but detectable anti-POR reactive proteins also in these same fractions, we believe this finding reflects some degree of contamination by microsomes—in hepatocytes, which are very abundant in rough and smooth ER—rather than some "liver-specific difference in organelle-targeting" which was not seen in lung, kidney or small intestine. By inducing CYP1A1 via TCDD or BNF pretreatment, this simply elevated the ratio of CYP1A1 to POR in liver mitochondria but did not decrease the amount of contamination of mitochondria by microsomes.

MT-Specificity of the Targeted CYP1A1 Protein. In the *mtp1A1* and *mtt1A1* lines, the MT-targeted CYP1A1 protein was detected only in mitochondrial fractions of kidney and small intestine

Molecular Pharmacology Fast Forward. Published on December 1, 2008 as DOI: 10.1124/mol.108.051888
This article has not been copyedited and formatted. The final version may differ from this version.

following TCDD, and in lung following BNF pretreatment. In *mtp1A1* and *mtt1A1* mice, trace amounts (~1-10%) of CYP1A1 could always be detected in microsomes from lung or liver after TCDD and from small intestine after BNF pretreatment (data not shown). The low level of CYP1A1 present in microsomes from TCDD- or BNF-pretreated *mtp1A1* and *mtt1A1* mice varied as a function of different inducers and tissues, suggesting that the NH_2-terminal signal sequence might not be absolute in effecting MT-targeting of the CYP1A1 protein in the intact animal. This conclusion is consistent with the finding that the protein kinase C (**PKC**)-mediated phosphorylation of Thr-35 in the nascent CYP1A1 peptide chain lowers the affinity for SRP binding—thus decreasing the amount of ER-targeting (Dasari et al., 2006). Considering the highly variable expression of PKC isoforms in different tissues and cell types (Yoshida et al., 1988;Webb et al., 2000;Blay et al., 2004) and the involvement of PKC in AHR-signaling pathways (Carrier et al., 1992;Long et al., 1998;Webb et al., 2000), PKC activity might contribute to the incomplete ablation of ER-targeted CYP1A1 in microsomes of some tissues, as seen in our MT-targeted mouse lines. Further studies are needed to understand the underlying mechanisms of tissue-specific CYP1A1 subcellular-targeting in the intact mouse and its physiological significance.

Oral BaP-Induced Immunosuppression is mc1A1-Dependent. Previous studies of mice receiving daily dietary BaP in our laboratories have demonstrated the importance of CYP1A1 in detoxication. In *Cyp1a1(-/-)* knockout mice, having no functional CYP1A1 protein in any tissue, daily oral BaP produced striking abnormalities within 18 days**:** loss in body weight, increased liver weight per total body weight, atrophy of the spleen and thymus, hypocellularity of the bone marrow with the lymphoid series particularly affected, elevated plasma ALT and AST levels, and evidence of anemia and increases in methemoglobin (Uno et al., 2004;Uno et al., 2006). These abnormalities were observed in the *mtp1A1* line (**Table 1**) but not in the *mc1A1* or *WT 1A1* mice—strongly

Molecular Pharmacology Fast Forward. Published on December 1, 2008 as DOI: 10.1124/mol.108.051888
This article has not been copyedited and formatted. The final version may differ from this version.

suggesting that the absence of microsomal CYP1A1 protein is the critical determinant in not allowing oral BaP detoxication to occur normally. Therefore, this study has established that the mc1A1 protein, and not the mt1A1 protein, is necessary and sufficient to support detoxication of BaP given orally to the intact mouse.

It should also be noted that, following daily oral BaP, absolute CYP1A1 mRNA levels in *mtp1A1* are higher than those in *mc1A1* or wild-type mice to a minor degree in small intestine, and more strikingly in both liver and spleen (**Fig. 6**). The significance of these observations is not known.

Differences in Up-Regulation of CYP1A2 and CYP1B1 mRNA. Intriguingly, the subcellular location of the CYP1A1 protein appeared to have an effect on CYP1A2 or CYP1B1 mRNA inducibility**;** moreover, this effect was tissue-specific. CYP1A2 mRNA levels are higher in *mtt1A1* and *mtp1A1* (compared with that in *mc1A1*) mice in small intestine following intraperitoneal TCDD pretreatment**;** in this regard, the MT-targeted lines are more similar to the *Cyp1a1(-/-)* knockout than the wild-type mouse (**Fig. 2A**, *bottom panel*). CYP1A2 mRNA levels are higher in *mtp1A1* (compared with that in *mc1A1*) mice in liver and spleen following administration of daily oral BaP**;** again, the MT-targeted line is more similar to the *Cyp1a1(-/-)* knockout mouse (**Fig. 6**, *middle right panels*). CYP1B1 mRNA levels are higher in *mtp1A1* (compared with that in *mc1A1*) mice in small intestine, liver and spleen following daily oral BaP**;** yet again, the MT-targeted line is more similar to the *Cyp1a1(-/-)* knockout mouse (**Fig. 6**, *bottom panels*). Hence, CYP1A2 and/or CYP1B1 mRNA accumulation requires either the presence of mitochondrial CYP1A1 (unlikely, because *WT 1A1* mice have mt1A1) or the absence of microsomal CYP1A1. Reasons for these fascinating observations are not understood and will require further experimentation.

How can we explain these “compensatory increases” in CYP1A2 and/or CYP1B1 mRNA when CYP1A1 is absent in one or the other organelle? Our analysis of basal CYP1 mRNA levels in the

Molecular Pharmacology Fast Forward. Published on December 1, 2008 as DOI: 10.1124/mol.108.051888
This article has not been copyedited and formatted. The final version may differ from this version.

organelle-specific *Cyp1a1* knock-in mouse lines suggests some interesting cross-talk exists between the *Cyp1* genes. This is particularly evident in small intestine, in which the CYP1B1 basal mRNA level is elevated in both *KO 1A1* and *mtp1A1* mice, whereas the CYP1A2 basal mRNA level is elevated only in *KO 1A1* mice. In previous studies (Uno et al., 2006;Uno et al., 2008) we have noted that compensatory up-regulation of one *Cyp1* family member ofttimes occurs in the absence of one or more of the other members. In the present study, we now find that the mitochondrial isoform of CYP1A1 apparently can compensate for CYP1A2, but not for CYP1B1, in the small intestine. The reason for this is unclear. Recent genomics research has uncovered multiple (currently poorly understood) mechanisms of genomic cross-talk. Perhaps the dynamic genome should be considered to be like a "community"**:** when one member of that community suddenly becomes absent (*e.g.* due to gene ablation), the rest of the genome decides which other members should raise or lower their levels of expression in order to compensate for that missing member. In liver of the untreated *Cyp1a2(-/-)* knockout mouse, for example, eleven genes became significantly up-regulated and 21 genes down-regulated (Smith et al., 2003).

Since publication of the **Enc**yclopedia **o**f **D**NA **E**lements (**ENCODE**) pilot project (The ENCODE Project Consortium, 2007), our lack of knowledge about the genome is more apparent than ever before. It is now realized how little is known about "what 'a gene' is", what mechanisms are involved in the cross-talk of *cis*- and *trans*-regulatory factors, how chromatin-remodeling and epigenetics affect gene expression, and why 60% of all (gene-rich and gene-desert) regions of the DNA chosen for the ENCODE study are incredibly conserved between pufferfish and mammals (Gerstein et al., 2007;Nebert et al., 2008). We can only conclude that there is much more to learn about compensatory up- and down-regulation of gene expression.

Conclusions. The generation of three knock-in mouse lines carrying CYP1A1 protein targeted

Molecular Pharmacology Fast Forward. Published on December 1, 2008 as DOI: 10.1124/mol.108.051888
This article has not been copyedited and formatted. The final version may differ from this version.

principally to the ER or the MT has been successful. Whether there are tissue- or cell-specific differences in the success of CYP1A1-protein organelle-targeting—or the tissue-specific dissimilarities represent minor problems in our ability to separate microsomes from mitochondrial (and vice versa) with absolute certainty—remains open to further study. Administration of daily dietary BaP to these knock-in mouse lines provided us with proof-in-principle, *i.e.* we conclude that the mc1A1 and not the mt1A1 is important in oral BaP detoxication and thus protection from the various forms of BaP-induced damage. We have also found striking increases in CYP1A2 and CYP1B1 mRNA up-regulation by oral BaP in the *mt1A1* (similar to that previously found in the *KO 1A1*) but not the *mc1A1* lines.

It would be desirable also to show a clinical effect that happens in *mtt1A1* and *mtp1A1* mice but not in *mc1A1* mice. Knowing that the LD_{50} for erythromycin in mice is 280 mg/kg, we gave doses of 28, 56 and 140 mg/kg to *WT 1A1*, *mc1A1*, *mtt1A1* and *mtp1A1* and watched for overt toxicity during the next 2 weeks**;** no differences were seen clinically, and no histological differences were observed in liver, lung, kidney, thymus, spleen or bone marrow. Because one or more enzymes of the CYP3A family are responsible for erythromycin metabolism (Tanaka, 1998), it is likely that mt1A1-mediated erythromycin metabolism is relatively minor compared with CYP3A-mediated metabolism. This is also likely to be true of other psychotropic drugs metabolized by mt1A1 (Anandatheerthavarada et al., 1999;Dasari et al., 2006).

Our reasons for the construction of these knock-in mouse lines include several hypotheses. First, our overriding assumption is that both ER- and MT-specific CYP1A1 function primarily for endogenous regulatory reasons (Nebert and Karp, 2008). ER-specific CYP1A1 might be important principally for the synthesis and degradation of critical life endogenous compounds and detoxication, as well as metabolic activation of various foreign chemicals entering the cell**;** this metabolism might

Molecular Pharmacology Fast Forward. Published on December 1, 2008 as DOI: 10.1124/mol.108.051888
This article has not been copyedited and formatted. The final version may differ from this version.

lead to genotoxicity and mutagenesis of the genomic DNA, carcinogenesis, and perhaps organ-specific toxicity. On the other hand, MT-specific CYP1A1 might be important principally for the synthesis and degradation of mitochondrial critical life endogenous compounds and the detoxication, as well as metabolic activation of various foreign chemicals entering the mitochondrion**;** such metabolism might lead to genotoxicity, mutagenesis of the mitochondrial DNA, apoptosis by way of the cytochrome *c* release-signaling pathway, and perhaps birth defects. One postulate—mc1A1, rather than mt1A1, being important in the detoxication of oral BaP—has been demonstrated in the present study. The remaining hypotheses will require additional work. These knock-in mouse lines are available to all interested colleagues.

Acknowledgments—We thank our colleagues for discussions and careful readings of this manuscript. These data were presented at the 26th (March 2006) and 27th (March 2007) Annual Meetings of the Society of Toxicology—in San Diego, CA, and Charlotte, NC, respectively. These studies were supported, in part, by NIH Grants R01 ES08147 (D.W.N.), R01 ES014403 (D.W.N.), R01 GM034883 (N.G.A.), and P30 ES06096 (T.P.D. & D.W.N.).

Molecular Pharmacology Fast Forward. Published on December 1, 2008 as DOI: 10.1124/mol.108.051888
This article has not been copyedited and formatted. The final version may differ from this version.

REFERENCES

Addya S, Anandatheerthavarada HK, Biswas G, Bhagwat SV, Mullick J and Avadhani NG (1997) Targeting of NH_2-terminal-processed microsomal protein to mitochondria**:** a novel pathway for the biogenesis of hepatic mitochondrial P450MT2. *J Cell Biol* **139:** 589–599.

Anandatheerthavarada HK, Addya S, Dwivedi RS, Biswas G, Mullick J and Avadhani NG (1997) Localization of multiple forms of inducible cytochromes P450 in rat liver mitochondria**:** immunological characteristics and patterns of xenobiotic substrate metabolism. *Arch Biochem Biophys* **339:** 136–150.

Anandatheerthavarada HK, Vijayasarathy C, Bhagwat SV, Biswas G, Mullick J and Avadhani NG (1999) Physiological role of the N-terminal processed P450 1A1 targeted to mitochondria in erythromycin metabolism and reversal of erythromycin-mediated inhibition of mitochondrial protein synthesis. *J Biol Chem* **274:** 6617–6625.

Araki K, Araki M, Miyazaki J and Vassalli P (1995) Site-specific recombination of a transgene in fertilized eggs by transient expression of Cre recombinase. *Proc Natl Acad Sci U S A* **92:** 160–164.

Bhagwat SV, Mullick J, Raza H and Avadhani NG (1999) Constitutive and inducible cytochromes P450 in rat lung mitochondria**:** xenobiotic induction, relative abundance, and catalytic properties. *Toxicol Appl Pharmacol* **156:** 231–240.

Blay P, Astudillo A, Buesa J M, Campo E, Abad M, Garcia-Garcia J, Miquel R, Marco V, Sierra M, Losa R, Lacave A, Brana A, Balbin M and Freije JM (2004) Protein kinase-Cθ is highly expressed in gastrointestinal stromal tumors, but not in other mesenchymal neoplasias. *Clin Cancer Res* **10:** 4089–4095.

Boopathi E, Anandatheerthavarada HK, Bhagwat SV, Biswas G, Fang JK and Avadhani NG (2000) Accumulation of mitochondrial P450MT2, NH_2-terminal truncated cytochrome P450 1A1 in rat brain during chronic treatment with β-naphthoflavone. A role in the metabolism of neuroactive drugs. *J Biol Chem* **275:** 34415–34423.

Boopathi E, Srinivasan S, Fang JK and Avadhani NG (2008) Bimodal targeting of proteins with chimeric signals and activation of cryptic mitochondrial-targeting signals by an inducible cytosolic endoprotease. *Mol Cell* **32:** 32–42.

Brown EG (1988) Mixed anionic detergent/aliphatic alcohol-polyacrylamide gel electrophoresis alters the separation of proteins relative to conventional sodium dodecyl sulfate-polyacrylamide gel electrophoresis. *Anal Biochem* **174:** 337–348.

Capecchi MR (1989) The new mouse genetics**:** altering the genome by gene targeting. *Trends Genet* **5:** 70–76.

Carrier F, Owens RA, Nebert DW and Puga A (1992) Dioxin-dependent activation of murine *Cyp1a1* gene transcription requires protein kinase C-dependent pPhosphorylation. *Mol Cell Biol* **12:** 1856–1863.

Chen Y, Yang Y, Miller ML, Shen D, Shertzer HG, Stringer KF, Wang B, Schneider SN, Nebert DW and Dalton TP (2007) Hepatocyte-specific *Gclc* gene deletion leads to rapid onset of steatosis with mitochondrial injury and liver failure. *Hepatology* **45:** 1118–1128.

Cheung C, Ma X, Krausz KW, Kimura S, Feigenbaum L, Dalton TP, Nebert DW, Idle JR and Gonzalez FJ (2005) Differential metabolism of 2-amino-1-methyl-6-phenylimidazo[4,5-*b*]pyridine (**PhIP**) in mice humanized for *CYP1A1* and *CYP1A2*. *Chem Res Toxicol* **18:** 1471–1478.

Chung JY, Kim JY, Kim WR, Lee SG, Kim YJ, Park JE, Hong YP, Chun YJ, Park YC, Oh S, Yoo KS, Yoo YH and Kim JM (2007) Abundance of aryl hydrocarbon receptor potentiates benzo[*a*]pyrene-induced apoptosis in Hepa-1c1c7 cells via CYP1A1 activation. *Toxicology* **235:** 62–72.

Dalton TP, Dieter MZ, Matlib RS, Childs NL, Shertzer HG, Genter MB and Nebert DW (2000) Targeted knockout of *Cyp1a1* gene does not alter hepatic constitutive expression of other genes in the mouse [*Ah*] battery. *Biochem Biophys Res Commun* **267:** 184–189.

Dasari VR, Anandatheerthavarada HK, Robin MA, Boopathi E, Biswas G, Fang JK, Nebert DW and Avadhani NG (2006) Role of protein kinase C-mediated protein phosphorylation in mitochondrial translocation of mouse CYP1A1, which contains a non-canonical targeting signal. *J Biol Chem* **281:** 30834–30847.

Derkenne S, Curran CP, Shertzer HG, Dalton TP, Dragin N and Nebert DW (2005) Theophylline pharmacokinetics**:** comparison of *Cyp1a1(-/-)* and *Cyp1a2(-/-)* knockout mice, humanized h*CYP1A1_1A2* knock-in mice lacking either the mouse *Cyp1a1* or *Cyp1a2* gene, and *Cyp1(+/+)* wild-type mice. *Pharmacogenet Genomics* **15:** 503–511.

Dragin N, Uno S, Wang B, Dalton TP and Nebert DW (2007) Generation of 'humanized' h*CYP1A1_1A2_Cyp1a1/1a2(-/-)* mouse line. *Biochem Biophys Res Commun* **359:** 635–642.

Foster RP and Wilson LD (1975) Purification and characterization of adrenodoxin reductase from bovine adrenal cortex. *Biochemistry* **14:** 1477–1484.

Garcia-Falcon MS, Gonzalez AS, Lage-Yusty MA, Lopez de Alda Villaizan MJ and Simal LJ (1996) Determination of benzo[*a*]pyrene in lipid-soluble liquid smoke (**LSLS**) by HPLC-FL. *Food Addit Contam* **13:** 863–870.

Genter MB, Clay CD, Dalton TP, Dong H, Nebert DW and Shertzer HG (2006) Comparison of mouse hepatic mitochondrial versus microsomal cytochromes P450 following TCDD treatment. *Biochem Biophys Res Commun* **342:** 1375–1381.

Gerstein MB, Bruce C, Rozowsky JS, Zheng D, Du J, Korbel JO, Emanuelsson O, Zhang ZD, Weissman S and Snyder M (2007) What is a gene, post-ENCODE? History and updated definition. *Genome Res* **17:** 669–681.

Gu H, Marth JD, Orban PC, Mossmann H and Rajewsky K (1994) Deletion of a DNA polymerase-β gene segment in T cells using cell type-specific gene targeting. *Science* **265:** 103–106.

Hankinson O (2005) Role of coactivators in transcriptional activation by the aryl hydrocarbon receptor. *Arch Biochem Biophys* **433:** 379–386.

Jiang Z, Dalton TP, Jin L, Wang B, Tsuneoka Y, Shertzer HG, Deka R and Nebert DW (2005) Toward the evaluation of function in genetic variability**:** characterizing human SNP frequencies and establishing BAC-transgenic mice carrying the human *CYP1A1_CYP1A2* locus. *Hum Mutat* **25:** 196–206.

Kawajiri K and Fujii-Kuriyama Y (2007) Cytochrome P450 gene regulation and physiological functions mediated by the aryl hydrocarbon receptor. *Arch Biochem Biophys* **464:** 207–212.

Kim HS, Kwack SJ and Lee BM (2000) Lipid peroxidation, antioxidant enzymes, and benzo[*a*]pyrene-quinones in the blood of rats treated with benzo[*a*]pyrene. *Chem Biol Interact* **127:** 139–150.

Li H, Witte DP, Branford WW, Aronow BJ, Weinstein M, Kaur S, Wert S, Singh G, Schreiner CM and Whitsett JA (1994) *Gsh4* encodes a LIM-type homeodomain, is expressed in the developing central nervous system, and is required for early postnatal survival. *EMBO J* **13:** 2876–2885.

Long WP, Pray-Grant M, Tsai JC and Perdew GH (1998) Protein kinase C activity is required for aryl hydrocarbon receptor pathway-mediated signal transduction. *Mol Pharmacol* **53:** 691–700.

Ma X, Idle JR, Malfatti MA, Krausz KW, Nebert DW, Chen CS, Felton S, Waxman DJ and Gonzalez FJ (2007) Mouse lung CYP1A1 catalyzes the metabolic activation of 2-amino-1-methyl-6-phenylimidazo[4,5-*b*]pyridine (**PhIP**).

Carcinogenesis **28:** 732–737.

Mansour SL, Thomas KR and Capecchi MR (1988) Disruption of the proto-oncogene *Int-2* in mouse embryo-derived stem cells**:** a general strategy for targeting mutations to non-selectable genes. *Nature* **336:** 348–352.

Meehan RR, Speed RM, Gosden JR, Rout D, Hutton JJ, Taylor BA, Hilkens J, Kroezen V, Hilgers J, Adesnik M, Friedberg T, Hastie ND and Wolf CR (1988) Chromosomal organization of the cytochrome *Cyp2c* gene family in the mouse**:** a locus associated with constitutive aryl hydrocarbon hydroxylase activity. *Proc Natl Acad Sci U S A* **85:** 2662–2666.

Nebert DW (1989) The [*Ah*] locus**:** genetic differences in toxicity, cancer, mutation, and birth defects. *Crit Rev Toxicol* **20:** 153–174.

Nebert DW and Dalton TP (2006) The role of cytochrome P450 enzymes in endogenous signalling pathways and environmental carcinogenesis. *Nat Rev Cancer* **6:** 947–960.

Nebert DW, Dalton TP, Okey AB and Gonzalez FJ (2004) Role of aryl hydrocarbon receptor-mediated induction of the CYP1 enzymes in environmental toxicity and cancer. *J Biol Chem* **279:** 23847–23850.

Nebert DW, Dalton TP, Stuart GW and Carvan MJ, III (2000a) "Gene-swap knock-in" cassette in mice to study allelic differences in human genes. *Ann N Y Acad Sci* **919:** 148–170.

Nebert DW and Gelboin HV (1968) Substrate-inducible microsomal aryl hydroxylase in mammalian cell culture. I. Assay and properties of induced enzyme. *J Biol Chem* **243:** 6242–6249.

Nebert DW and Karp CL (2008) Endogenous functions of the aryl hydrocarbon receptor**:** intersection of cytochrome P450 (**CYP1**)-metabolized eicosanoids and AHR biology. *J Biol Chem* **283:** in press

Nebert DW, Roe AL, Dieter MZ, Solis WA, Yang Y and Dalton TP (2000b) Role of the aromatic hydrocarbon receptor and [*Ah*] gene battery in the oxidative stress response, cell cycle control, and apoptosis. *Biochem Pharmacol* **59:** 65–85.

Nebert DW and Russell DW (2002) Clinical importance of the cytochromes P450. *Lancet* **360:** 1155–1162.

Nebert DW, Zhang G and Vesell ES (2008) From human genetics and genomics to pharmacogenetics and pharmacogenomics**:** past lessons, future directions. *Drug Metab Rev* **40:** 187–224.

Nelson DR, Zeldin DC, Hoffman SM, Maltais LJ, Wain HM and Nebert DW (2004) Comparison of cytochrome P450 (*CYP*) genes from the mouse and human genomes, including nomenclature recommendations for genes, pseudogenes and alternative-splice variants. *Pharmacogenetics* **14:** 1–18.

Niranjan BG, Avadhani NG and DiGiovanni J (1985) Formation of benzo[*a*]pyrene metabolites and DNA adducts catalyzed by a rat liver mitochondrial monooxygenase system. *Biochem Biophys Res Commun* **131:** 935–942.

Park JY, Shigenaga MK and Ames BN (1996) Induction of cytochrome P450 1A1 by 2,3,7,8-tetrachlorodibenzo-*p*-dioxin or indolo[2,3-*b*]carbazole is associated with oxidative DNA damage. *Proc Natl Acad Sci U S A* **93:** 2322–2327.

Puga A, Tomlinson CR and Xia Y (2005) Ah receptor signals cross-talk with multiple developmental pathways. *Biochem Pharmacol* **69:** 199–207.

Raza H and Avadhani NG (1988) Hepatic mitochondrial cytochrome P-450 system. Purification and characterization of two distinct forms of mitochondrial cytochrome P-450 from β-naphthoflavone-induced rat liver. *J Biol Chem* **263:** 9533–9541.

Robinson JR, Felton JS, Levitt RC, Thorgeirsson SS and Nebert DW (1975) Relationship between "aromatic hydrocarbon responsiveness" and the survival times in mice treated with various drugs and environmental compounds. *Mol Pharmacol* **11:** 850–865.

Smith AG, Davies R, Dalton TP, Miller ML, Judah D, Riley J, Gant T and Nebert DW (2003) Intrinsic hepatic phenotype associated with the *Cyp1a2* gene as shown by cDNA expression microarray analysis of the knockout mouse. *EHP Toxicogenomics* **111:** 45–51.

Tanaka E (1998) Clinical importance of non-genetic and genetic cytochrome P450 function tests in liver disease. *J Clin Pharm Ther* **23:** 161–170.

The ENCODE Project Consortium (2007) Identification and analysis of functional elements in 1% of the human genome by the ENCODE pilot project. *Nature* **447:** 799–816.

Uno S, Dalton TP, Derkenne S, Curran CP, Miller ML, Shertzer HG and Nebert DW (2004) Oral exposure to benzo[*a*]pyrene in the mouse**:** detoxication by inducible cytochrome P450 is more important than metabolic activation. *Mol Pharmacol* **65:** 1225–1237.

Uno S, Dalton TP, Dragin N, Curran CP, Derkenne S, Miller ML, Shertzer HG, Gonzalez FJ and Nebert DW (2006) Oral benzo[*a*]pyrene in *Cyp1* knockout mouse lines**:** CYP1A1 important in detoxication, CYP1B1 metabolism required for immune damage independent of total-body burden and clearance rate. *Mol Pharmacol* **69:** 1103–1114.

Uno S, Dalton TP, Shertzer HG, Genter MB, Warshawsky D, Talaska G and Nebert DW (2001) Benzo[*a*]pyrene-induced toxicity**:** paradoxical protection in *Cyp1a1(-/-)* knockout mice having increased hepatic BaP-DNA adduct levels. *Biochem Biophys Res Commun* **289:** 1049–1056.

Uno S, Dragin N, Miller ML, Dalton TP, Gonzalez FJ and Nebert DW (2008) Basal and inducible CYP1 mRNA quantitation and protein localization throughout the mouse gastrointestinal tract. *Free Radic Biol Med* **44:** 570–583.

Webb BL, Hirst SJ and Giembycz MA (2000) Protein kinase C isoenzymes**:** review of their structure, regulation and role in regulating airways, smooth muscle tone, and mitogenesis. *Br J Pharmacol* **130:** 1433–1452.

Wells PG, Bhuller Y, Chen CS, Jeng W, Kasapinovic S, Kennedy JC, Kim PM, Laposa RR, McCallum GP, Nicol CJ, Parman T, Wiley MJ and Wong AW (2005) Molecular and biochemical mechanisms in teratogenesis involving reactive oxygen species. *Toxicol Appl Pharmacol* **207:** 354–366.

Xu DX, Wang JP, Sun MF, Chen YH and Wei W (2006) Lipopolysaccharide down-regulates the expression of intestinal pregnane X receptor and cytochrome P450 *Cyp3a11*. *Eur J Pharmacol* **536:** 162–170.

Yoshida Y, Huang FL, Nakabayashi H and Huang KP (1988) Tissue distribution and developmental expression of protein kinase C isozymes. *J Biol Chem* **263:** 9868–9873.

Molecular Pharmacology Fast Forward. Published on December 1, 2008 as DOI: 10.1124/mol.108.051888
This article has not been copyedited and formatted. The final version may differ from this version.

FOOTNOTES

Correspondence should be addressed to**:** Department of Environmental Health, University of Cincinnati Medical Center, P.O. Box 670056, Cincinnati OH 45267-0056, Tele 513-821-4664; Fax 513-821-4664; email dan.nebert@uc.edu

These studies were supported, in part, by NIH Grants R01 ES08147 (D.W.N.), R01 ES014403 (D.W.N.), R01 GM034883 (N.G.A.), and P30 ES06096 (T.P.D. & D.W.N.).

Molecular Pharmacology Fast Forward. Published on December 1, 2008 as DOI: 10.1124/mol.108.051888
This article has not been copyedited and formatted. The final version may differ from this version.

FIGURE LEGENDS

Fig. 1. Generation of three *Cyp1a1* knock-in mouse lines. ***A***, Scheme showing the wild-type (***WT***) *Cyp1a1* gene (*top line*), targeting construct carrying the organelle-specific alterations (*2nd line*), targeted *Cyp1a1* alleles after removal of the *TK* gene (*3rd line)*, and the final targeted alleles (*bottom line*) after the *NEO* gene had been removed via Cre-mediated recombination to create the *Cyp1a1(mc), Cyp1a1(mtt)* and *Cyp1a1(mtp)* alleles. *NEO* (G418-resistant mini-cassette) and *TK* (thymidine kinase mini-cassette) represent genes used as selectable markers. *Closed rectangles* denote the seven exons**;** exon 2 (where ATG translation start-site is located) spans 851 bp. The ATG start-site for translation (denoted as *vertical line & horizontal arrow*) is located 15 nucleotides into exon 2. Exon 2 insertions (*bold arrows pointing to striped rectangles*, not drawn completely to scale) represent the organelle-specific variations. *Eco*RV and *Eag*I sites and the inserted *loxP* sites (*orientation* denoted by *small arrow heads*) are shown. ***B***, NH_2-terminal chimeric signal sequences of CYP1A1 proteins encoded by *Cyp1a1* genes targeted with organelle-specific variations**:** WT 1A1 = wild-type**;** mc1A1 = ER-specific targeting**;** mtt1A1 = mitochondrial truncated targeting**;** mtp1A1 = mitochondrial proteolysis targeting. The altered residues are *outlined* in *grey*. ***C***, Southern blot analysis. Genomic DNA from 129/SvJ mouse ES cell colonies was digested with *Eco*RV endonuclease followed by hybridization with the probe shown upstream of exon 1 in panel ***A*** (*3rd line*). The 8.6- and 3.8-kb bands represent the *Cyp1a1* wild-type and targeted (*mc*, *mtt*, and *mtp*) alleles, respectively. ***D***, PCR analysis of genomic DNA for the *Cyp1a1* wild-type and targeted (*mc*, *mtt*, and *mtp*) alleles. Positions of the primers in intron 2 are shown in panel ***A*** (*bottom line*).

Fig. 2. Tissue mRNA levels. CYP1A1 and CYP1A2 mRNA levels were determined by qRT-PCR in mouse tissues after treatment with TCDD (***A***, 15 μg/kg i.p. for 3 consecutive days) or BNF (***B***, 80 mg/kg i.p. for 10 consecutive days). The CYP1A1 mRNA levels from corn-oil treated *WT 1A1* mice in each tissue were set as "1.0 control", and relative mRNA levels are expressed as fold-increases on a logarithmic scale**;** note values on the Y-axis vary over a >10,000-fold range. The mouse lines are noted at *bottom***:** *WT 1A1*, *mc1A1*, *mtt1A1*, *mtp1A1* and *KO 1A1*. **ND**, CYP1A1 mRNA was nondetectable. The mRNA levels are expressed relative to β-actin mRNA levels**;** thus, values within a tissue, but not between tissues, can be compared. Data are reported as means ± S.E.M. of four mice per group. ***P* <0.05, when compared with mRNA levels of CYP1A1 in *WT* mice following the same treatment. $^{\dagger}P$ <0.05, compared with mRNA levels of CYP1A2 in *WT* mice following the same treatment.

Fig. 3. Western immunoblot analysis of subcellular localization of CYP1A1 proteins. Mitochondrial (**MT**) and ER (*i.e.* microsomes) fractions (***A***) and cytosolic fractions (***B***) were isolated and resolved by SDS-PAGE or MAD-PAGE. Designation of the mouse lines, with or without TCDD or BNF treatment, noted at *top*, is the

Molecular Pharmacology Fast Forward. Published on December 1, 2008 as DOI: 10.1124/mol.108.051888
This article has not been copyedited and formatted. The final version may differ from this version.

same as that in **Fig. 2**. Across each row, CYP1A1, POR (ER marker), PHB (MT marker), and GCLM (cytosolic marker) proteins were detected using antibodies. Protein loadings (μg per lane) for the CYP1A1 immunoblots are noted in *parentheses***;** 20 μg of protein from subcellular fractions was loaded for the detection of the ER and MT markers**;** 30 μg of protein was loaded for detection of the cytosolic marker. K, kidney. Liv, liver. S.I., small intestine. Lg, lung.

Fig. 4. Mitochondrial versus microsomal enzyme activities in BNF-treated and untreated mice. ***A***, Erythromycin *N*-demethylase (**ERND**) is expressed as the rate of HCHO formation in nmol per min per mg protein. Inhibition of ERND activity by prior addition of α-FDX1 or SKF-525A was carried out as described previously (Anandatheerthavarada et al., 1997;Anandatheerthavarada et al., 1999). ***P* <0.05, when hepatic mitochondrial ERND activity from BNF-treated *mtt1A1* or *mtp1A1* mice is compared with that from BNF-treated *WT 1A1* mice. ***B***, BaP hydroxylase activity is expressed in pmol 3- plus 9-hydroxyBaP/min/mg protein. Note the different values on the Y-axis in all panels. Data are reported as means ± S.E.M. (N = 3 or 4 mice per group). Designation of mouse lines is same as that in **Fig. 2**. ***P* <0.01, when microsomal BaP hydroxylase from BNF-treated *WT 1A1* or *mc1A1* is compared with that from untreated *WT 1A1* mice. $^{\dagger}P$ <0.05, when microsomal BaP hydroxylase from BNF-treated *mtp1A1* is compared with that from untreated *WT 1A1* mice.

Fig. 5. Whole blood BaP levels following continuous oral BaP. Whole blood was collected, as described, from mice receiving oral BaP 125 mg/kg/day for 5 days. Data are reported as means ± S.E.M. of four mice per group. Designation of mouse lines is the same as that in **Fig. 2**. ***P* <0.01, when compared with levels in *mc1A1* or *WT 1A1* mice. The *bracket* denotes that BaP levels in *KO 1A1* mice are significantly greater (*P* <0.01) than those in *mtp1A1* mice.

Fig. 6. CYP1 mRNA levels following 18 days of continuous oral BaP (125 mg/kg/day). The CYP1A1 mRNA levels from corn-oil treated *WT 1A1* mice in each tissue were set as "1.0 control", and relative mRNA levels are expressed as fold-increases on a logarithmic scale**;** note values on the Y-axis vary over a >1000-fold range. **ND**, nondetectable. The mRNA levels are expressed relative to β-actin mRNA levels**;** thus, values within a tissue, but not between tissues, can be compared. Data are reported as means ± S.E.M. of four mice per group. Designation of mouse lines is the same as that in **Fig. 2**. ***P* <0.05, when compared with mRNA levels for that gene in BaP-treated *WT 1A1* mice. $^{\dagger}P$ <0.05, when compared with mRNA levels for that gene in corn oil-treated *WT 1A1* mice.

TABLE 1

Effect of oral BaP on body weight, organ weight, liver enzymes, hematocrit, hemoglobin, and peripheral blood cell types

	Corn oil only				**BaP**			
***Cyp1a1*:**	***WT***	***mc***	***mtp***	***KO***	***WT***	***mc***	***mtp***	***KO***
Body weight (g, gained or lost)	+0.8 ± 0.5	+0.6 ± 0.3	+1.6 ± 0.5	+1.0 ± 0.4	+0.7 ± 0.2	+1.1 ± 0.3	–1.3 ± 0.3*	–2.7 ± 0.5*
Liver weight (mg/g body weight)	47 ± 4.1	46 ± 2.0	47 ± 0.9	47 ± 2.2	41 ± 1.1	42 ± 1.3	53 ± 2.2*	55 ± 2.3*
Spleen weight (mg/g body weight)	3.8 ± 0.2	3.9 ± 0.1	3.6 ± 0.1	3.5 ± 0.1	3.4 ± 0.1	3.1 ± 0.2	2.0 ± 0.1*	1.2 ± 0.1*†
Thymus weight (mg/g body weight)	1.6 ± 0.3	1.6 ± 0.1	1.6 ± 0.4	2.3 ± 0.4	1.5 ± 0.1	1.5 ± 0.2	0.5 ± 0.04*	0.2 ± 0.04*†
ALT (I.U./L)	33 ± 6.9	26 ± 6.1	18 ± 3.2	21 ± 2.1	21 ± 4.2	41 ± 3.1	48 ± 5.1*	53 ± 3.7*
AST (I.U./L)	105 ± 18	115 ± 16	105 ± 16	81 ± 6.8	76 ± 1.9	84 ± 16	98 ± 1.5*	93 ± 1.8*
Hematocrit (%)	52 ± 1.0	52 ± 0.5	53 ± 1.1	52 ± 0.5	53 ± 2.8	52 ± 1.1	45 ± 1.2*	38 ± 1.0*†
Total hemoglobin (mM)	6.9 ± 0.6	7.3 ± 0.3	7.3 ± 0.4	6.8 ± 0.3	6.9 ± 0.2	7.2 ± 0.6	6.2 ± 0.3*	6.1 ± 0.1*
Methemoglobin (%)	2.2 ± 0.9	1.0 ± 0.2	1.2 ± 0.5	1.4 ± 0.4	1.3 ± 0.2	0.9 ± 0.2	2.4 ± 0.2*	4.9 ± 0.5*
Peripheral Blood								
Neutrophils (%)	24 ± 4.7	24 ± 1.8	21 ± 4.0	22 ± 4.1	20 ± 4.2	19 ± 3.2	43 ± 4.2*	42 ± 3.3*
Lymphocytes (%)	78 ± 5.3	73 ± 5.4	77 ± 4.6	78 ± 4.4	76 ± 4.4	82 ± 4.0	52 ± 5.7*	53 ± 2.1*

Mice (N=4 per group) were fed corn oil-soaked food or BaP-soaked food (125 mg/kg/day) for 18 days. Values are expressed as means ± S.E.M.

*****P <0.05, when compared with BaP-treated *WT 1A1* wild-type mice. †P <0.05, when compared with BaP-treated *mtp1A1* mice.

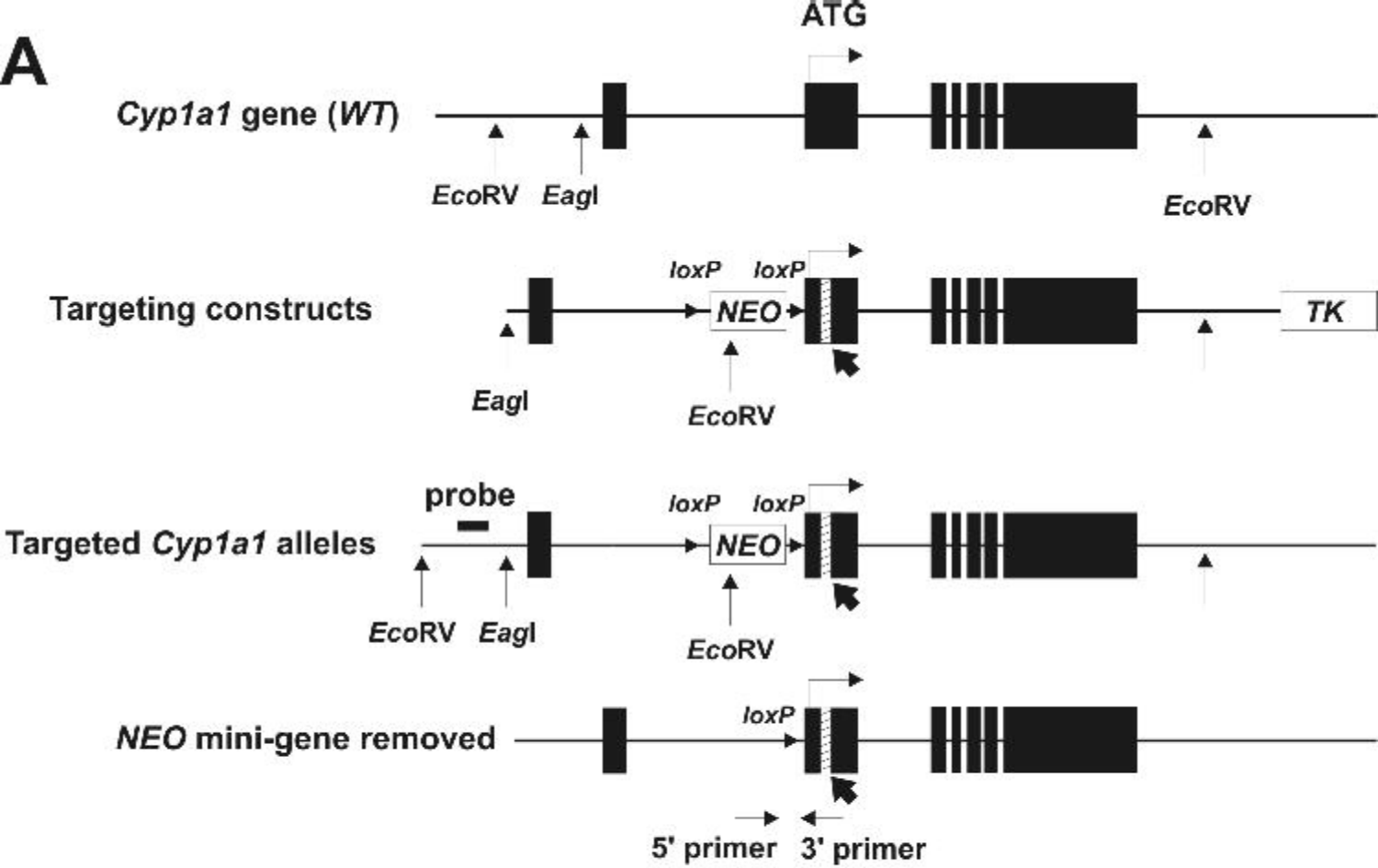
A
ATG
Cyp1a1 gene (WT)
EcoRV
EagI
EcoRV
Targeting constructs
loxP
loxP
NEO
TK
EagI
EcoRV
probe
Targeted Cyp1a1 alleles
loxP
loxP
NEO
EcoRV
EagI
EcoRV
NEO mini-gene removed
loxP
5' primer
3' primer

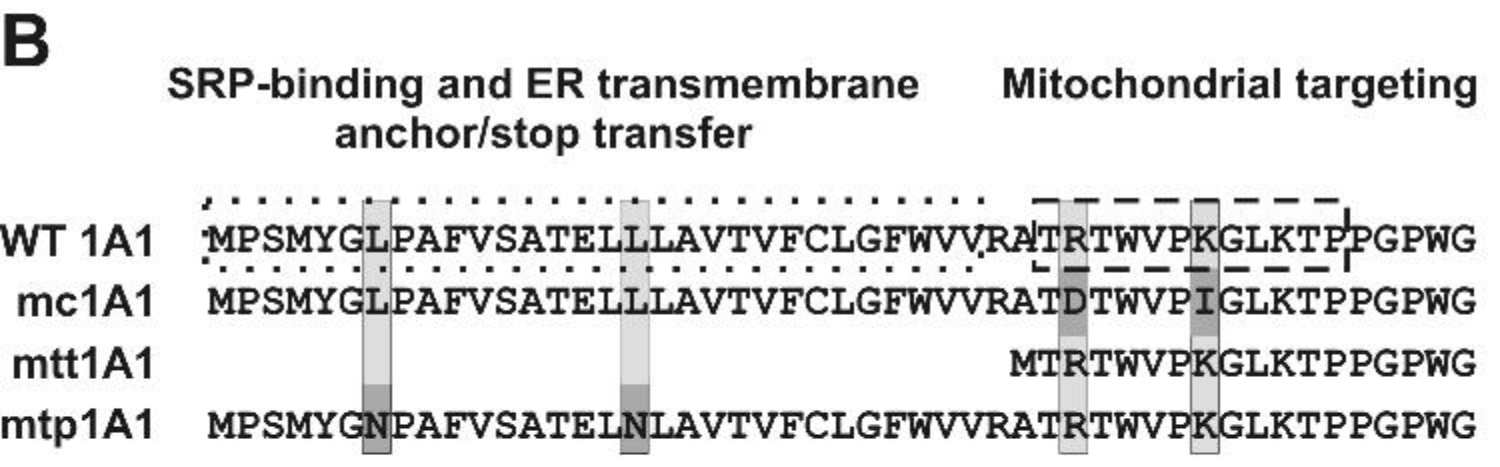
B
SRP-binding and ER transmembrane anchor/stop transfer
Mitochondrial targeting
WT 1A1 MPSMYGLPAFVSATELLLAVTVFCLGFWVVRATRTWVPKGLKTPPGPWG
mc1A1 MPSMYGLPAFVSATELLLAVTVFCLGFWVVRATDTWVPIGLKTPPGPWG
mtt1A1 MTRTWVPKGLKTPPGPWG
mtp1A1 MPSMYGNPAFVSATELNLAVTVFCLGFWVVRATRTWVPKGLKTPPGPWG

Figure 1

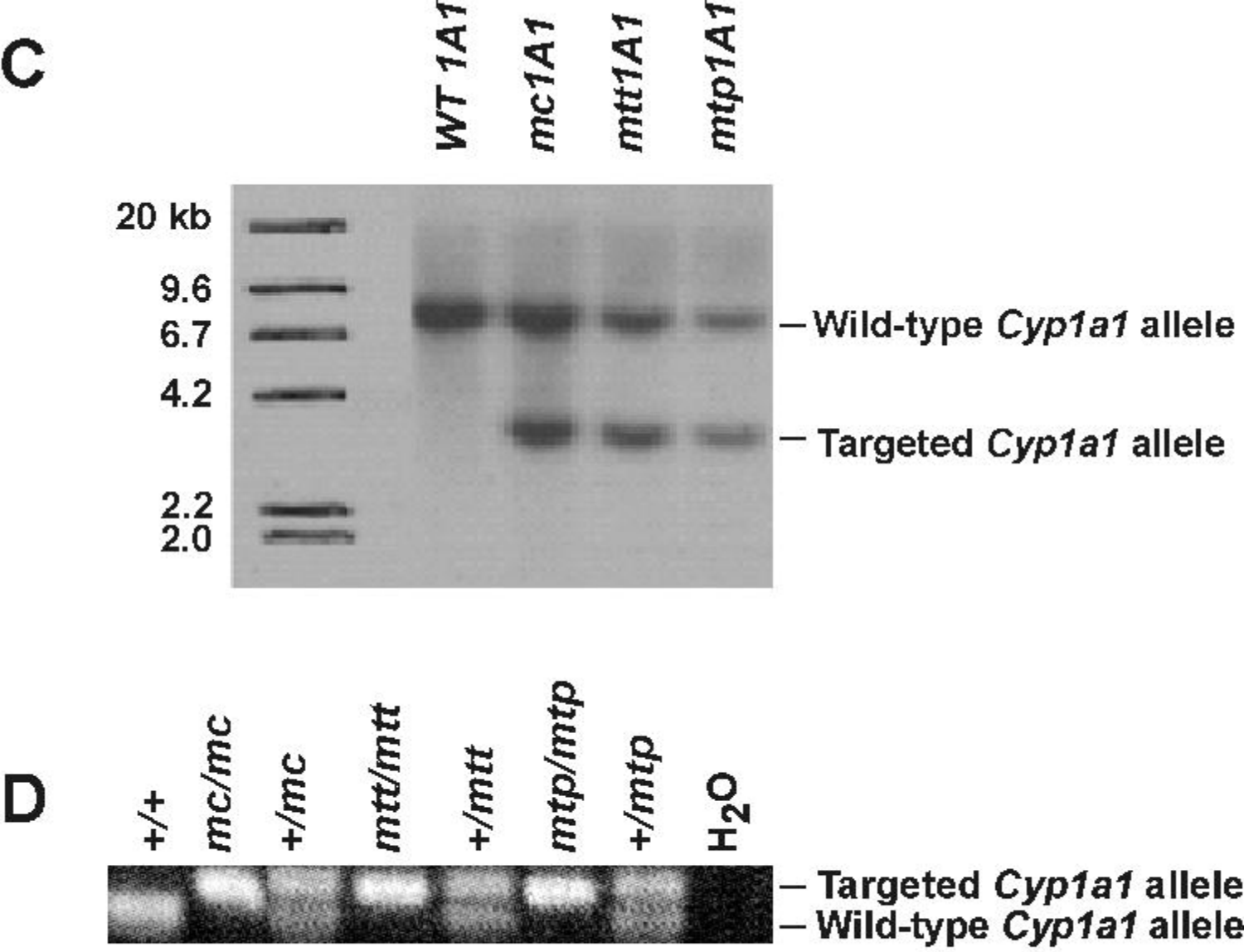
C
WT 1A1
mc1A1
mtt1A1
mtp1A1
20 kb
9.6
6.7
4.2
2.2
2.0
Wild-type Cyp1a1 allele
Targeted Cyp1a1 allele
D
+/+
mc/mc
+/mc
mtt/mtt
+/mtt
mtp/mtp
+/mtp
H2O
Targeted Cyp1a1 allele
Wild-type Cyp1a1 allele

Figure 1

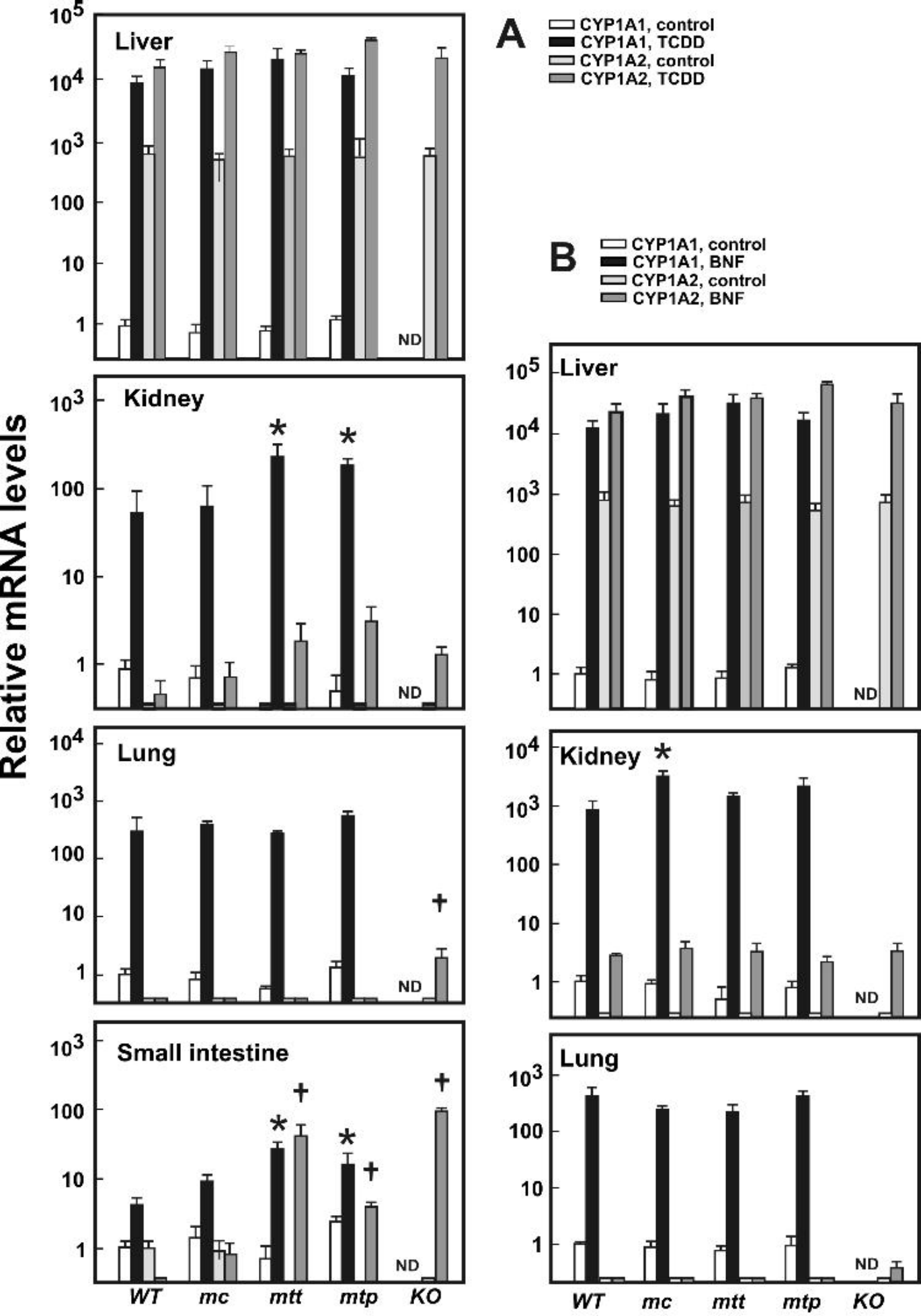
A
CYP1A1, control
CYP1A1, TCDD
CYP1A2, control
CYP1A2, TCDD
B
CYP1A1, control
CYP1A1, BNF
CYP1A2, control
CYP1A2, BNF
Relative mRNA levels
Liver
Kidney
Lung
Small intestine
ND
*
†
WT
mc
mtt
mtp
KO

Figure 2

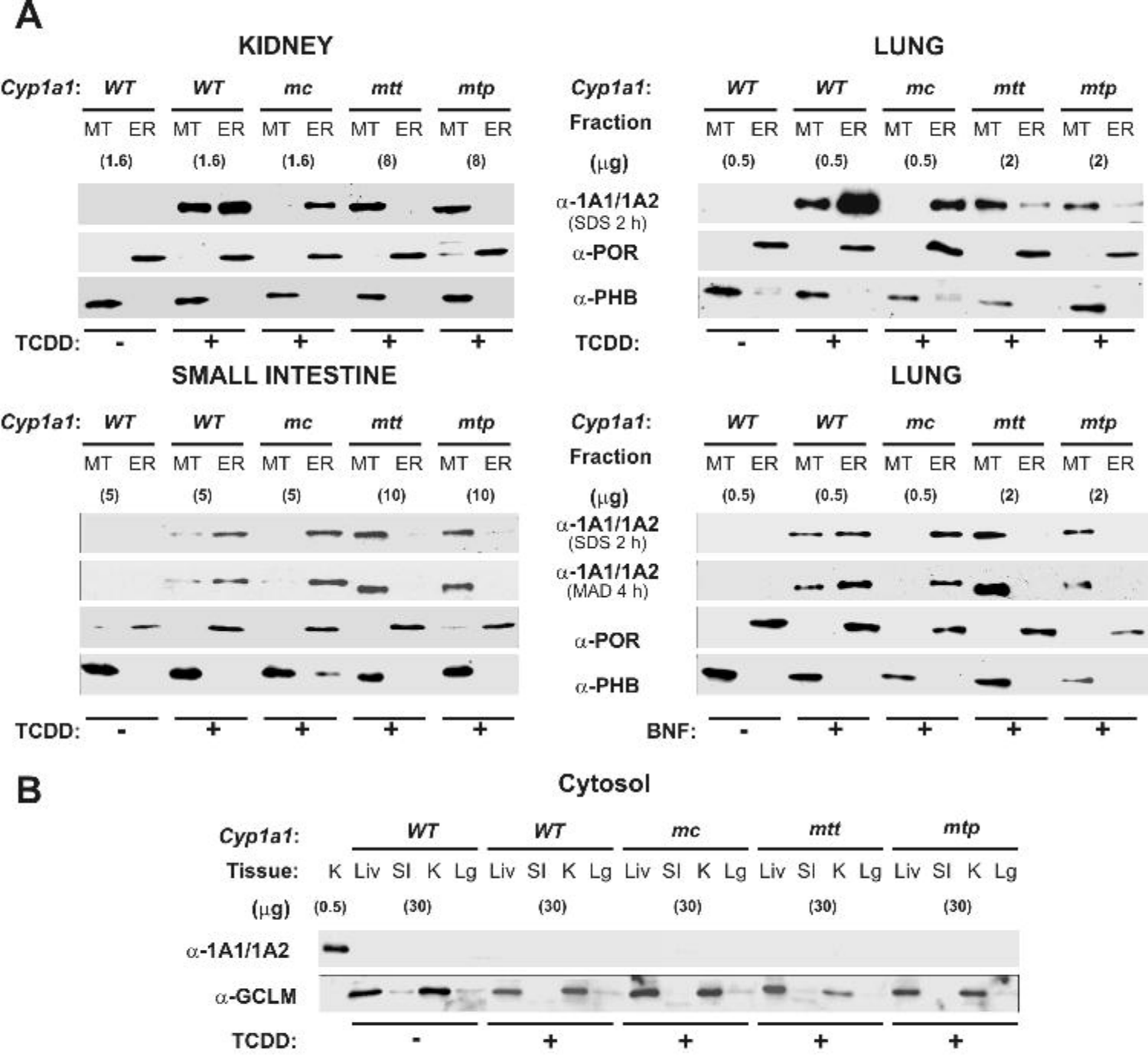
A
KIDNEY
LUNG
Cyp1a1: WT WT mc mtt mtp
Fraction
MT ER MT ER MT ER MT ER MT ER
(μg)
(1.6) (1.6) (1.6) (8) (8)
(0.5) (0.5) (0.5) (2) (2)
α-1A1/1A2
(SDS 2 h)
α-POR
α-PHB
TCDD: - + + + +
SMALL INTESTINE
LUNG
(5) (5) (5) (10) (10)
α-1A1/1A2
(MAD 4 h)
BNF: - + + + +
B
Cytosol
Tissue: K Liv SI K Lg Liv SI K Lg Liv SI K Lg Liv SI K Lg Liv SI K Lg
(0.5) (30) (30) (30) (30) (30)
α-1A1/1A2
α-GCLM

Figure 3

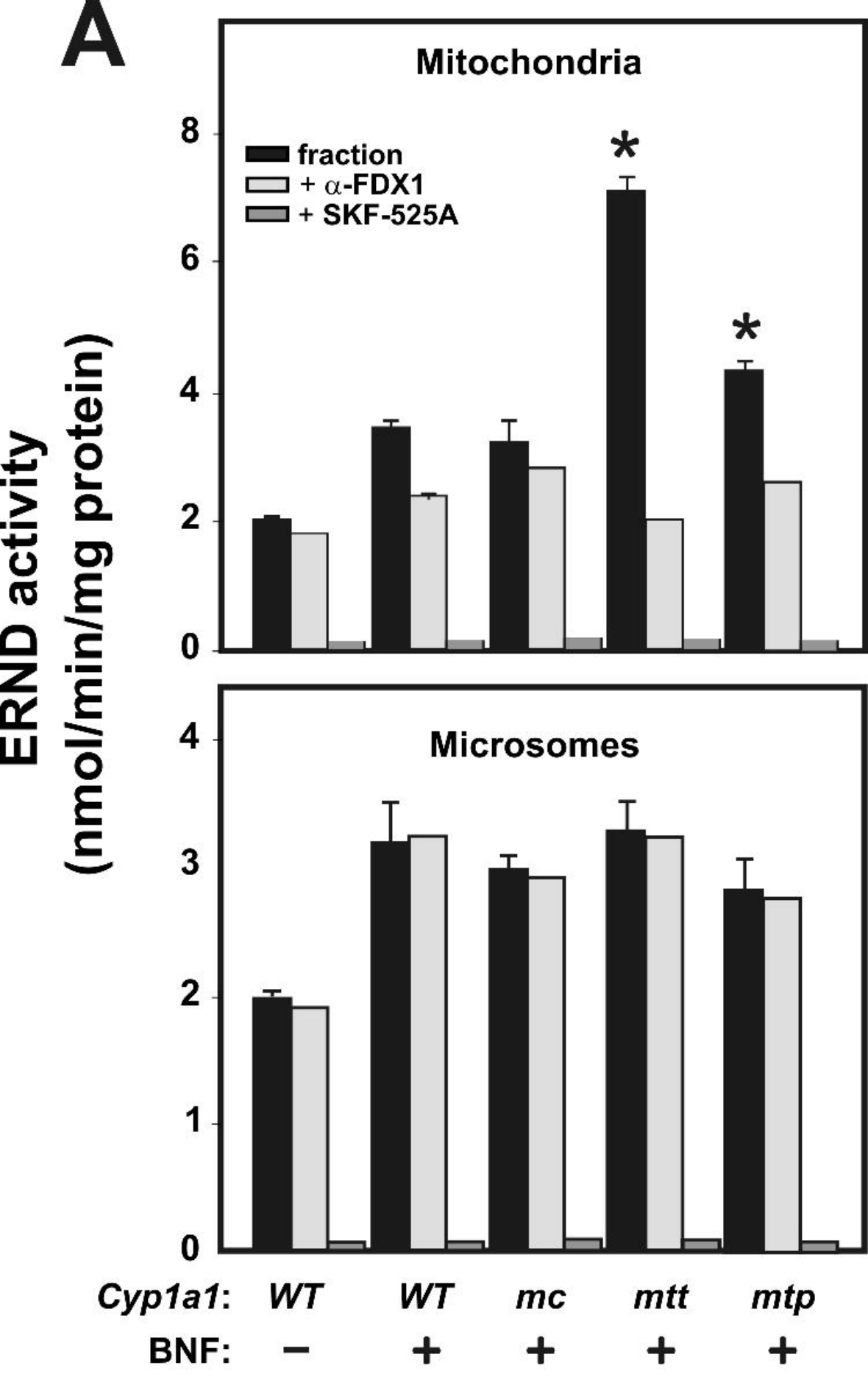
A
Mitochondria
fraction
+ α-FDX1
+ SKF-525A
*
*
8
6
4
2
0
Microsomes
4
3
2
1
0
ERND activity
(nmol/min/mg protein)
Cyp1a1: WT WT mc mtt mtp
BNF: − + + + +

Figure 4

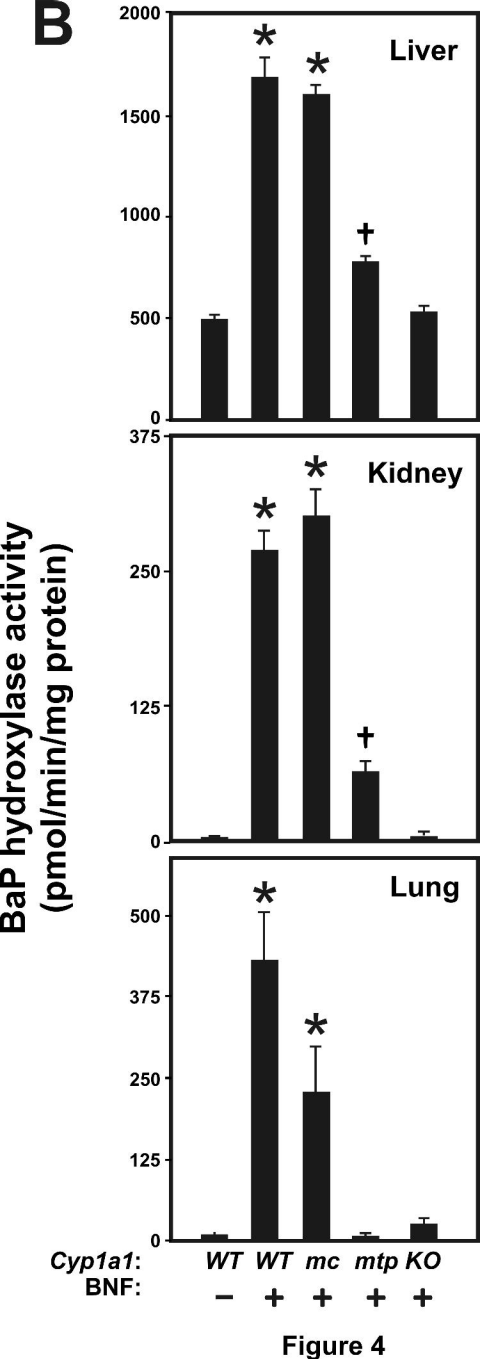
B
Liver
Kidney
Lung
BaP hydroxylase activity
(pmol/min/mg protein)
2000
1500
1000
500
0
375
250
125
0
500
375
250
125
0
*
+
Cyp1a1:
BNF:
WT WT mc mtp KO
– + + + +

Figure 4

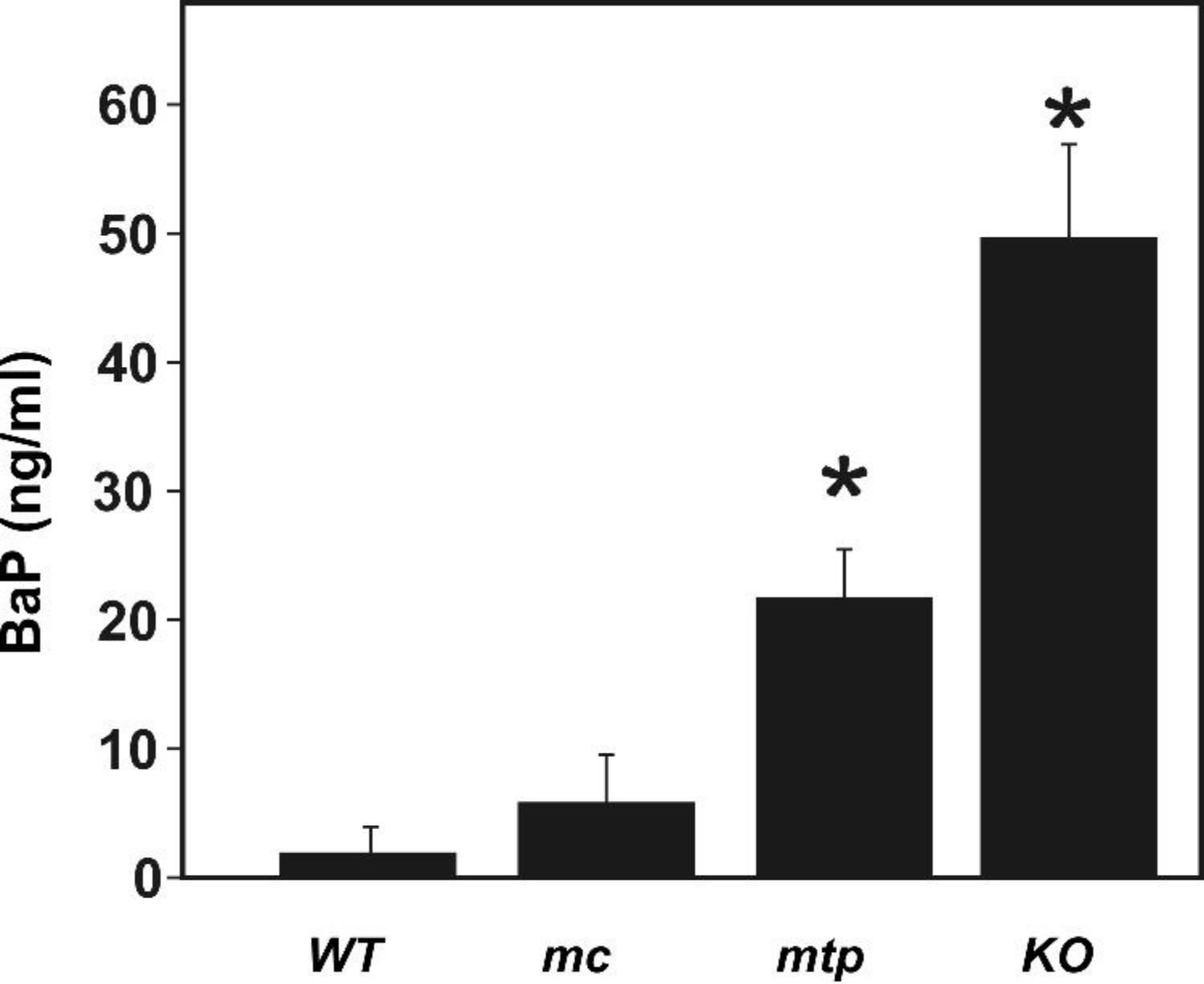

Figure 5

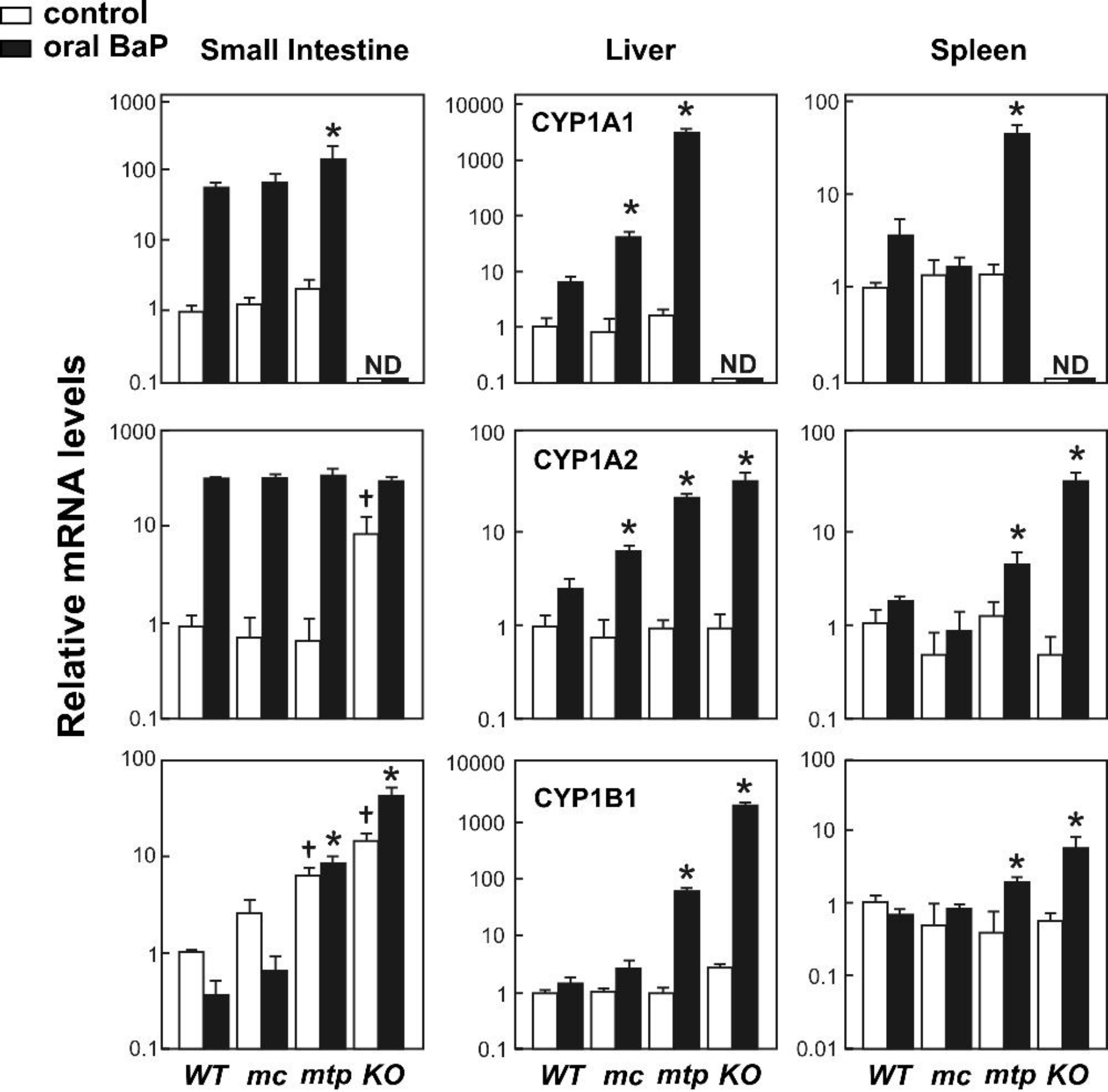
control
oral BaP
Small Intestine
Liver
Spleen
Relative mRNA levels
CYP1A1
CYP1A2
CYP1B1
ND
*
†
WT
mc
mtp
KO

Figure 6